

## Review

---

# Applications of differential thermal analysis to the preparation of single crystals

Dietrich Schultze

*Analytical Center Berlin-Adlershof, Institute for Physical Chemistry, D-1199 Berlin (Germany)*

(Received 29 January 1991)

## Abstract

Studies utilizing differential thermal analysis (DTA) to investigate the growth of single crystals are reviewed. Most such studies have dealt with equilibrium phenomena: melting and solid–solid transformations of compounds to be grown as single crystals; and phase diagrams (liquid–solid equilibria) of systems to determine congruently melting compositions and concentration and temperature intervals for the growth of bulk crystals or epitaxial layers from high-temperature solutions. Non-equilibrium phenomena that interfere with the equilibrium ones listed above can also be investigated by means of DTA: the formation and transitions of metastable phases; and the undercooling and delay of the nucleation and/or growth of crystals. Further possible applications of DTA measurements in relation to the growth and investigation of single crystals are outlined and the usefulness of the DTA method is evaluated.

## INTRODUCTION

The techniques of single crystal growth are based on the phase transformation from the liquid (molten or dissolved) or gaseous state to the solid state. Hence the equilibria and kinetics of these transformations are of fundamental importance in terms of the technique and conditions used to grow single crystals. The differential thermal analysis (DTA) technique (in the cooling mode) can be used as a model of the crystal growth process or (in the heating mode) its reverse. Besides this obvious use, DTA can be used to investigate the growth of single crystals of compounds in a much wider sense.

DTA can be used to (i) obtain information on the synthesis of starting materials in order to optimize their preparation; (ii) determine the melting and solid–solid transformation temperatures of a compound (treated as a single-component system) so that the appropriate growth technique and temperature regime can be selected; (iii) construct phase diagrams (multi-

---

Presented at the Forum of Thermoanalysts, Prague, 1990.

component systems) which can then be used to detect new compounds and to characterize their melting behaviour and suitable growth conditions; (iv) find accurate liquidus and solidus temperatures in systems forming non-stoichiometric compounds in order to determine exactly the congruently melting composition, to optimize the composition of the starting material, and to improve the purity and perfection of the crystals; (v) find the liquidus and solidus temperatures of systems forming solid solutions; (vi) make liquidus (i.e. solubility) measurements on flux systems (high temperature solutions) in order to determine the temperature and concentration required to grow bulk crystals or epitaxial films; (vii) provide information on the supercooling of melts or solutions before the onset of crystallization; (viii) make vapour pressure measurements in order to determine suitable temperature and pressure conditions for growing decomposable compounds; and (ix) study single crystals in order to identify new phases, determine the transformation temperatures (e.g. the Curie or Néel temperature) of crystals, characterize solid solutions (e.g. doped crystals) in terms of their melting or transformation behaviour, and characterize the purity and perfection of the crystals.

This review covers the items (ii) to (vii). In the above the term DTA has been used, even in cases where the terms quantitative DTA or heat-flux differential scanning calorimetry (DSC) would have been more accurate. Of course, power-compensating DSC can provide analogous results in relation to single-crystal growth, but this technique has not found such wide applications as DTA due to its restricted temperature range.

## THE MELTING AND TRANSFORMATION OF COMPOUNDS

The temperature and character (congruent or incongruent) of melting of a compound and the occurrence or non-occurrence of solid-state transformations are decisive factors in choosing the appropriate growth technique and apparatus design. Single crystals of a congruently melting compound which does not decompose or transform in the solid state are best grown from the melt of the compound. The DTA diagram suggests this route of preparation because there are no thermal transformations between ambient and melting temperatures. Such behaviour has been observed and confirmed by successive experiments on growing crystals of fresnoite ( $\text{Ba}_2\text{TiSi}_2\text{O}_8$ ) [1],  $\text{La}_3\text{Ga}_5\text{SiO}_{14}$  [2],  $\text{Pb}_5\text{SiV}_2\text{O}_{12}$  [3],  $\text{Bi}_{12}\text{SiO}_{20}$  [4],  $\text{Zn}_3\text{Nb}_2\text{O}_8$  [5], and most of the  $\text{Ti}_3\text{BX}_4$  compounds (B = V, Nb or Ta; X = S or Se; except for  $\text{Ti}_3\text{VS}_4$ ) [6]. Using DTA heating and cooling curves, Pastor [7] found that ammonium dihydrogen phosphate (ADP) can be molten and crystallized quasi-congruently, if contained in a small sealed vessel to suppress the evaporation of water and ammonia. Consequently, Bridgman-type crystal-growth experiments proved successful. Analogously,  $\text{CsH}_2\text{AsO}_4$  and solid solutions of  $\text{Cs}(\text{H}_{1-x}\text{D}_x)_2\text{AsO}_4$  can be melted congruently in closed ampoules. However,

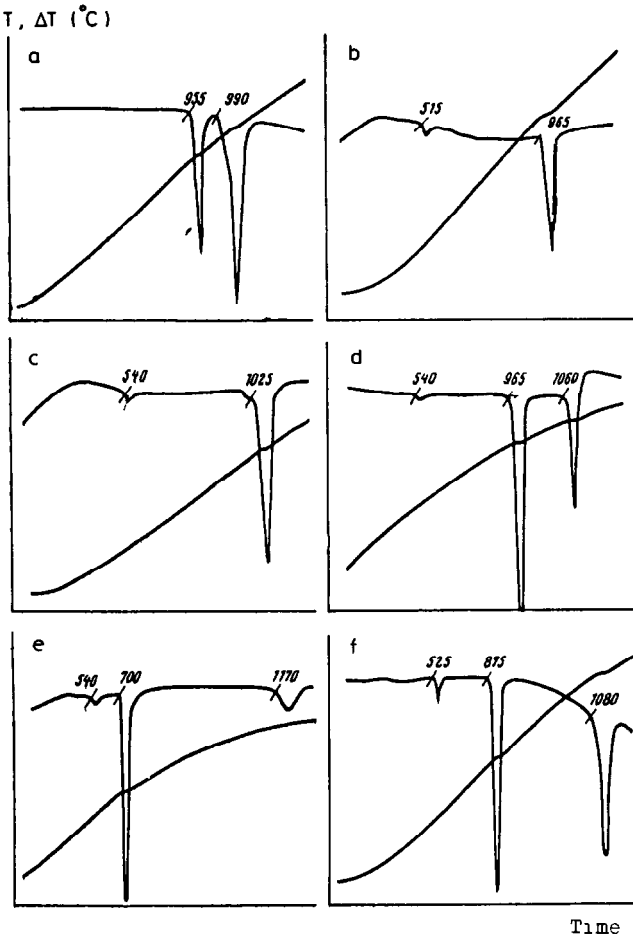


Fig 1 DTA curves of caesium-rare earth molybdates  $\text{CsRE}(\text{MoO}_4)_2$  RE = (a) La, (b) Pr; (c) Dy, (d) Ho, (e) Lu; (f) Y From Vinokurov and Klevtsov [9]

the preparation of single crystals of these compounds is prohibited by solid-state transformations above room temperature [8].

Vinokurov and Klevtsov [9] found that, of the series of caesium-rare-earth (RE) molybdates,  $\text{CsRE}(\text{MoO}_4)_2$ , (Fig. 1), those with RE = Pr to Dy give only one strong DTA peak at their melting temperature and, consequently, can be grown from their melts. (A small DTA effect between 500 and 550°C in all these binary molybdates could not be interpreted from X-ray diffraction measurements and does not affect the preparation of single crystals.) However, solid-state transformations between ambient and melting temperature would cause a deterioration of crystal quality or even total failure of crystal growth from the melt. Caesium-rare-earth molybdates with RE = La, Ho to Lu, and Y exhibit a phase transformation in the solid state, which is indicated by another and stronger DTA effect and results in

multiple cracking of the crystals after growth. This group of molybdates can be grown as single crystals by other techniques, e.g. from a flux, but not from their own melt.

Whether a crystal underlying a solid-state transformation will be damaged upon cooling depends on the nature of this transformation and the specific properties of the crystal. Reconstructive transformations will cause a deterioration of the crystal and crystals can be easily undercooled resulting, at room temperature, in a metastable crystal of the high-temperature type. A crystal may survive a displacive, rotational, or dilatational transformation, but will contain many imperfections, dislocations or strains. DTA can be used to elucidate the transformation pathway and, eventually, to determine suitable growth conditions and treatment of the crystals. For example, gadolinium molybdate ( $\text{Gd}_2(\text{MoO}_4)_3$ ) has two stable phases  $\alpha$  (below  $850^\circ\text{C}$ ) and  $\beta$  (above  $850^\circ\text{C}$ ) [10]. DTA studies have shown that the transformation  $\alpha \rightarrow \beta$  which occurs on heating proceeds rapidly, but the reverse transformation which occurs on cooling cannot be detected. The  $\beta$  modification can be cooled metastably to  $160^\circ\text{C}$  without any defect formation in the crystals. At  $160^\circ\text{C}$  a paraelectric-ferroelectric transformation occurs and the crystal becomes polydomenic. This transformation is readily reversible. Conclusions drawn from this thermal behaviour are that single crystals of  $\beta\text{-Gd}_2(\text{MoO}_4)_3$  grown from the melt should not be cooled too slowly, especially just below  $850^\circ\text{C}$ , otherwise transformation to  $\alpha\text{-Gd}_2(\text{MoO}_4)_3$  will occur. Annealing below  $850^\circ\text{C}$  is inappropriate. Around  $160^\circ\text{C}$  the crystal should be cooled slowly, and special precautions must be taken to suppress domain formation.

Sodium nitrate (m.p.  $312^\circ\text{C}$ ) exhibits a  $\lambda$  type transformation at  $270^\circ\text{C}$ . Single crystals of sodium nitrate, when grown from the melt, must be annealed for a long time in this temperature region in order to prevent cracking. Nevertheless, melt-grown crystals contain many more strains and dislocations than solution-grown crystals and are unsuitable for use in optical applications.

Cracking of  $\text{Ag}_4\text{P}_2\text{O}_7$  single crystals (m.p.  $570^\circ\text{C}$ ) after growth from the melt, related to a phase transformation at  $350^\circ\text{C}$ , can be suppressed by pulling in [210] direction and slow cooling through the transformation interval [11]. Single crystal growth of rare earth trifluorides from their respective melts by the pulling (Czochralski) or ampoule (Bridgman) techniques frequently suffered from solid-solid transformations. Contradictory data have been obtained on the polymorphism in the  $\text{REF}_3$  series by DTA investigations [12–14]. These discrepancies could be explained by an extreme sensitivity against impurities, e.g. rare earth oxide fluorides REOF even at concentrations in the order of 0.1 mol% [15] or alkaline earth fluorides [16]. These admixtures form solid solutions with anion vacancies in the  $\text{REF}_3$  thus stabilizing the tysonite ( $\text{LaF}_3$  type) modification. The polymorphism of pure rare earth trifluorides is illustrated in Fig. 2. One may

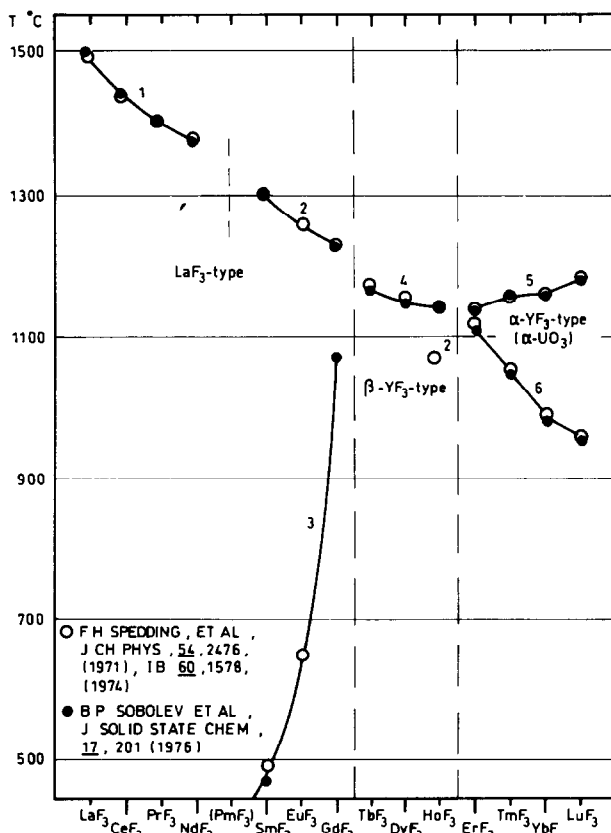


Fig 2 Polymorphic transformations and melting temperatures of rare earth trifluorides REF<sub>3</sub>. Reprinted with the permission of Academic Press from Sobolev et al [16]

predict that RE<sub>3</sub> single crystals can be grown from their melts without complications if RE represents La to Nd, and Tb, Dy, and Ho. DTA with careful exclusion of water vapour and crystal growth experiments in a hydrogen fluoride atmosphere [14] have confirmed this and show that GdF<sub>3</sub> single crystals can also be obtained without impurity conditioned transformation.

In the rare earth trichloride series only TbCl<sub>3</sub>, DyCl<sub>3</sub> and HoCl<sub>3</sub> are known to be dimorphic. The transformation (readily observed by DTA in TbCl<sub>3</sub> only) results in twinning and cracking of melt-grown crystals [17]. No transformation is observed by DTA upon cooling of DyCl<sub>3</sub> and HoCl<sub>3</sub>, because of a high activation energy for the transformation. Accordingly metastable single crystals of the high-temperature modification of DyCl<sub>3</sub> and HoCl<sub>3</sub> can be obtained from the melts of these compounds. The polymorphic transformation to the stable low-temperature modification is facilitated by admixtures, as has been shown by DTA studies of the systems DyCl<sub>3</sub>-GdCl<sub>3</sub> and HoCl<sub>3</sub>-TbCl<sub>3</sub>. Extrapolating the transformation temperature to 0% admixtures allows the calculation of the transformation temper-

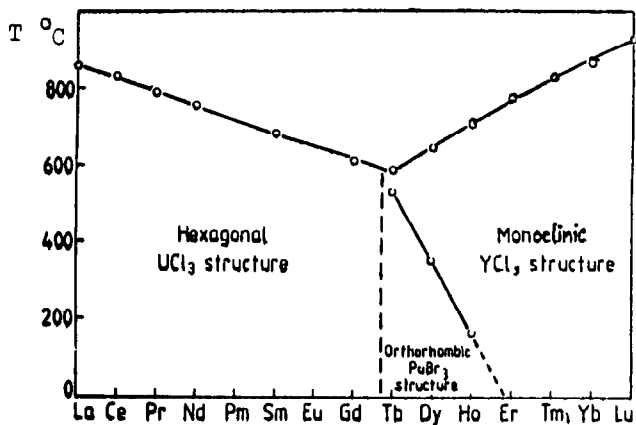


Fig 3. Polymorphic transformations and melting temperatures of rare earth trichlorides,  $RECl_3$ . Reprinted with the permission of Pergamon Press PLC from Garton and Walker [17].

atures for pure  $DyCl_3$  and  $HoCl_3$  and a structural diagram for the  $RECl_3$  series to be constructed (Fig. 3).

The DTA phase diagrams of  $BaF_2-REF_3$  [18] show congruently melting compounds ( $BaRE_2F_8$ ) for  $RE = Ho$  to  $Lu$  and  $Y$ . A phase transformation some 30–40 K below the melting point was detected for the  $Yb$  and  $Lu$  compounds and was suspected in the others. Nevertheless, because the high- and low-temperature modifications are closely related crystallochemically, and because the phase transformation occurs at sufficiently high a temperature that defect healing can occur, single crystals of good optical quality can be grown [19] from the melts of  $BaEr_2F_8$ ,  $Ba(Yb, Ho)_2F_8$  and  $Ba(Yb, Er)_2F_8$ .

It was concluded from the DTA measurements that both  $BaDy_2F_8$  and  $BaHo_2F_8$  melt incongruently and cannot be grown from their melts, whereas single crystals of congruently melting  $BaY_2F_8$ ,  $BaEr_2F_8$ ,  $BaDyYF_8$  and  $BaErYF_8$  can be prepared by means of the Bridgman technique [20].

#### INCONGRUENT MELTING AND PHASE-DIAGRAM STUDIES

If a substance melts incongruently, i.e. under the formation of another higher melting compound or a gas phase, the growth of single crystals from a melt of the same composition is difficult or even impossible. Incongruent melting is indicated on a DTA diagram by an additional thermal effect: melting occurs in two steps, i.e. at the peritectic and liquidus temperatures. Usually there is no total re-equilibration upon cooling. Therefore the DTA cooling curve and the DTA reheating curve are not simply the reverse and repetition of the initial heating curve. Reactions in which a gas phase is involved are best followed by using simultaneous thermogravimetric (TG) investigations.

Mill' et al. [21] investigated various ternary germanates ( $M_3^{2+}M_2^{3+}Ge_3O_{12}$ ;  $M^{2+} = Ca, Mn, Sr$  or  $Cd$ ;  $M^{3+} = Ga, Cr, V, Fe, Mn, Rh, Sc$  or  $In$ ) having a

garnet structure and melting points below 1500 °C (which is the maximum working temperature for platinum crucibles) as possible substitutes for  $\text{Gd}_3\text{Ga}_5\text{O}_{12}$  (GGG, m.p. = 1740 °C). A TG-DTA study of these compounds showed that only  $\text{Ca}_3\text{Ga}_2\text{Ge}_3\text{O}_{12}$  is a suitable substitute for GGG. The cadmium compounds melted congruently but with evaporation of CdO; the other compounds were unstable in air, decomposed before melting or melted above 1500 °C. A previous DTA investigation of  $\text{Ca}_3\text{Ga}_2\text{Ge}_3\text{O}_{12}$  had shown that this compound melts congruently at 1380 °C at stoichiometric composition [22]. Besides this garnet phase, Mill' et al. [23] also found two other congruently melting ternary compounds in the ternary oxide system  $\text{CaO}-\text{Ga}_2\text{O}_3-\text{GeO}_2$ , namely  $\text{Ca}_2\text{Ga}_2\text{GeO}_7$  and  $\text{Ca}_3\text{Ga}_2\text{Ge}_{4+x}\text{O}_{14+2x}$  ( $x = 0$  to 1). Single crystals of these compounds (with  $x = 0$  for the latter) were prepared by pulling from the melt. The latter compound is closely related to  $\text{La}_3\text{Ga}_5\text{SiO}_{14}$  and its solid solutions ( $(\text{La}_{1-x}\text{Nd}_x)_3\text{Ga}_5\text{SiO}_{14}$ ) which were found, by means of DTA, to melt congruently and to exhibit no transformation at temperatures above room temperature, so that single crystals could be grown easily from the melt [2].

The DTA investigation of the  $\text{Gd}_2\text{O}_3-\text{MoO}_3$  melting diagram made by Megumi et al. [24] revealed (Figs. 4(a) and 4(b)) one congruently melting compound  $\text{Gd}_2(\text{MoO}_4)_3 = \text{Gd}_2\text{O}_3 \cdot 3\text{MoO}_3$  (m.p. = 1157 °C), incongruently melting  $\text{Gd}_2\text{O}_3 \cdot 4\text{MoO}_3$  and  $\text{Gd}_2\text{O}_3 \cdot 6\text{MoO}_3$ , and refractory  $\text{Gd}_2\text{O}_3 \cdot \text{MoO}_3$ , for which the melting characteristics could not be determined. The inclusion of  $\text{Gd}_2\text{O}_3 \cdot \text{MoO}_3$  in single crystals of  $\text{Gd}_2(\text{MoO}_4)_3$  is caused by the nearness of the liquidus  $\leq 1157$  °C) and eutectic (1150 °C) temperatures at  $\text{Gd}_2\text{O}_3$  concentrations of 25–39 mol% and the high vapour pressure of  $\text{MoO}_3 \cdot \beta\text{-Gd}_2(\text{MoO}_4)_3$  formed by crystallization from the melt should cause a transformation to  $\alpha\text{-Gd}_2(\text{MoO}_4)_3$  which is stable below 850 °C. This transformation, however, is highly retarded, as discussed previously, and gives rise to metastable  $\beta\text{-Gd}_2(\text{MoO}_4)_3$ . These results suggest that single crystals of  $\beta\text{-Gd}_2(\text{MoO}_4)_3$  should be grown from a melt containing a small excess of  $\text{MoO}_3$  to compensate for evaporation losses, and under carefully controlled constant temperature in order to hinder crystallization of the  $\text{Gd}_2(\text{MoO}_4)_3-\text{Gd}_2\text{O}_3 \cdot \text{MoO}_3$  eutectic. Crystals of other compounds present in the system cannot be grown by means of the Czochralski technique.

If the compositions of an incongruently melting compound and a melt in equilibrium with it at the melting temperature (peritectic point) are similar, it is possible to grow crystals using the Czochralski or Bridgman techniques and starting with a melt that is slightly off-stoichiometric in the lower-melting sense. When growing crystals of a truly congruently melting compound this deviation from stoichiometry is unnecessary and should be avoided in order to avoid the formation of inclusions. Therefore it is very important to know exactly whether or not a compound does melt congruently. Careful DTA studies can be used to obtain this information.

From their DTA investigations, Ivanova et al. [25] concluded that all the

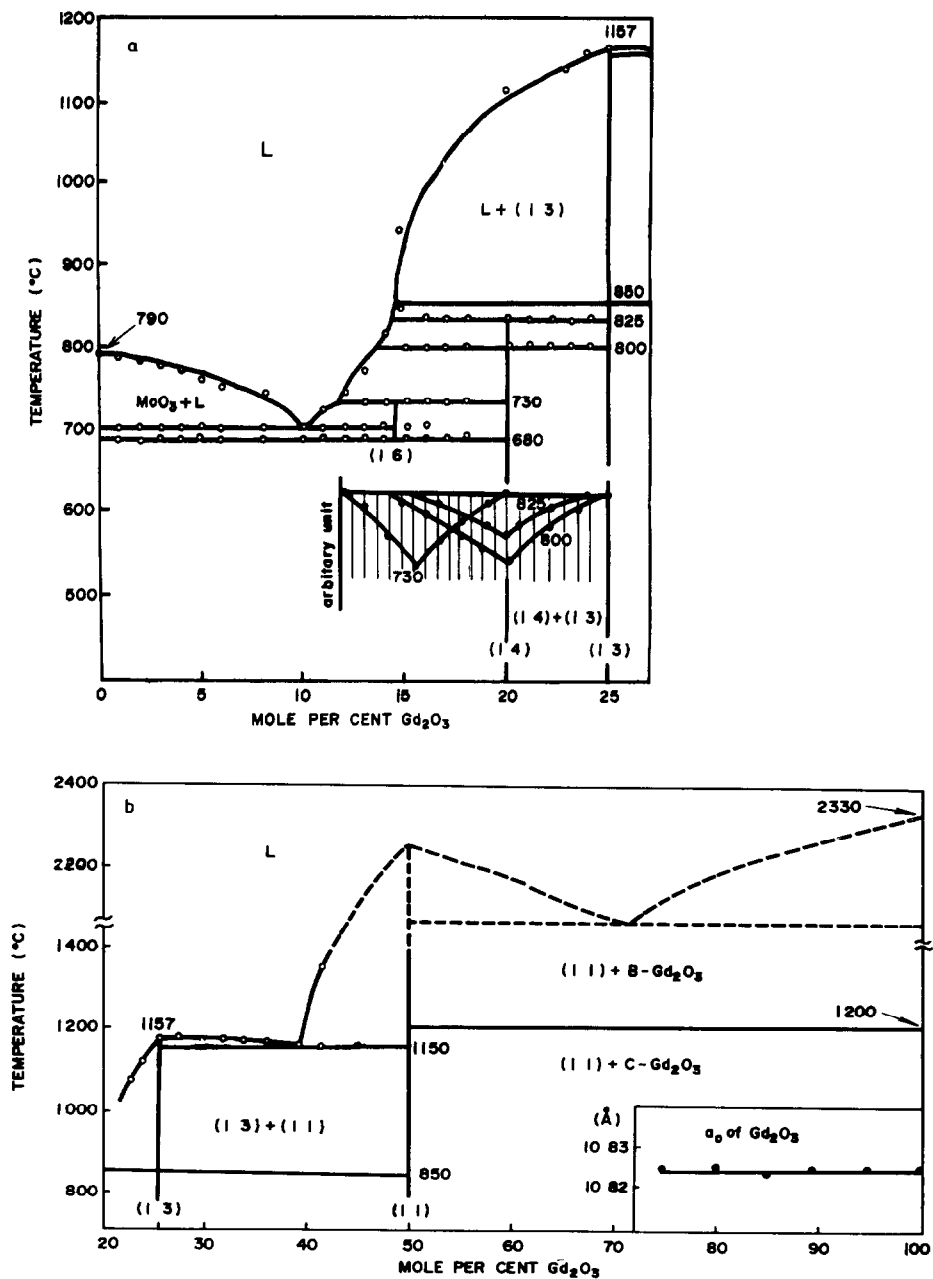


Fig 4 Equilibrium diagram for the  $Gd_2O_3$ - $MoO_3$  system. (a)  $MoO_3$ - $Gd_2(MoO_4)_3$  section (b)  $Gd_2(MoO_4)_3$ - $Gd_2O_3$  section Reprinted with the permission of Pergamon Press PLC from Megumi et al. [24].

binary lithium rare earth fluorides  $LiREF_4$  ( $RE = La$  to  $Lu$  and  $Y$ ) melt incongruently. Conversely, Pastor et al. [26] demonstrated that  $LiErF_4$ ,  $LiHoF_4$  and the solid solution  $LiY_{0.428}Er_{0.500}Tm_{0.067}Ho_{0.005}F_4$  melt con-

gruently if a reactive atmosphere (hydrogen fluoride–helium mixture) is applied in order to prevent hydrolysis. However, even traces of water desorbed from the platinum crucible cause hydrolysis of the melt, as indicated by the occurrence of a eutectic DTA effect when heating a sample in a second run. Safi et al. [27] compared the DTA curves of  $\text{LiY}_{0.434}\text{Er}_{0.500}\text{Tm}_{0.055}\text{Ho}_{0.011}\text{F}_4$  before and after pre-heating in normal air to show the effect of hydrolysis. Whereas the untreated material exhibited one narrow melting peak for the  $\text{LiREF}_4$  solid solution, thermally treated  $\text{LiREF}_4$  gave one sharp effect at a lower temperature, characteristic of the  $\text{LiF}$ – $\text{LiREF}_4$  eutectic, followed by a broader melting peak. This observation confirms that pyrohydrolysis is responsible for the decomposition of  $\text{LiREF}_4$  into  $\text{LiF}$  and oxidic phases.

A further investigation of the  $\text{LiF}$ – $\text{ErF}_3$  and  $\text{LiF}$ – $\text{LuF}_3$  systems by Harris et al. [28] with careful exclusion of oxygen and water confirmed that both  $\text{LiErF}_4$  and  $\text{LiLuF}_4$  do melt congruently with eutectics on either side of the respective compounds  $\text{LiREF}_4$ . With the  $\text{LiF}$ – $\text{YF}_3$  system difficulties arise due to the higher reactivity of the melts towards the container materials and due to the similarity of the composition of the  $\text{YF}_3$  rich eutectic (51 mol%  $\text{YF}_3$ ) and the composition of  $\text{LiYF}_4$ . Here the authors [28] presumed either congruent or possibly syntectic melting (decomposition into two immiscible liquids between the eutectic temperature and the homogeneous liquidus temperature), depending on the level of contamination. In good agreement with these results,  $\text{LiErF}_4$  and  $\text{LiLuF}_4$  crystals could be pulled from stoichiometric melts or melts containing a small excess or shortage of  $\text{LiF}$ . Problems with the seeding of  $\text{LiYF}_4$  crystals are ascribed to the deviating behaviour of the composition.

DTA and X-ray diffraction studies of the phase diagram for the  $\text{K}_2\text{O}$ – $\text{Nb}_2\text{O}_5$  system [29] have shown that  $\text{KNbO}_3$  melts incongruently, the peritectic composition being similar to the stoichiometric composition. A later more detailed study of this system [30] (Fig. 5) has confirmed the character of the phase diagram with a peritectic composition of 50.5–51 mol%  $\text{K}_2\text{O}$ , but liquidus temperatures had to be corrected to be 15–45 K higher. There exists a melting-point maximum at 56 mol%  $\text{K}_2\text{O}$  due to another, possibly metastable, as yet unknown compound. Using these results,  $\text{KNbO}_3$  single crystals were successfully pulled from a melt with a slight excess (51.7–52.8 mol%) at  $\text{K}_2\text{O}$  [31].

An earlier DTA study of the quasibinary section  $\text{K}_2\text{MoO}_4$ – $\text{Nd}_2(\text{MoO}_4)_3$  suggested the existence of two congruently melting compounds, namely  $\text{KNd}(\text{MoO}_4)_2$  and  $\text{K}_5\text{Nd}(\text{MoO}_4)_4$  [32]. Experiments on the latter compound have shown that single crystals of optical quality can be grown from the melt, but with difficulty due to the steep temperature gradient and the slow pulling rate required. This behaviour and the results of DTA investigations suggest incongruent melting [33]. A later DTA and X-ray study of the  $\text{K}_2\text{MoO}_4$ – $\text{Nd}_2(\text{MoO}_4)_3$  section by Evdokimov et al. [34] confirmed incon-

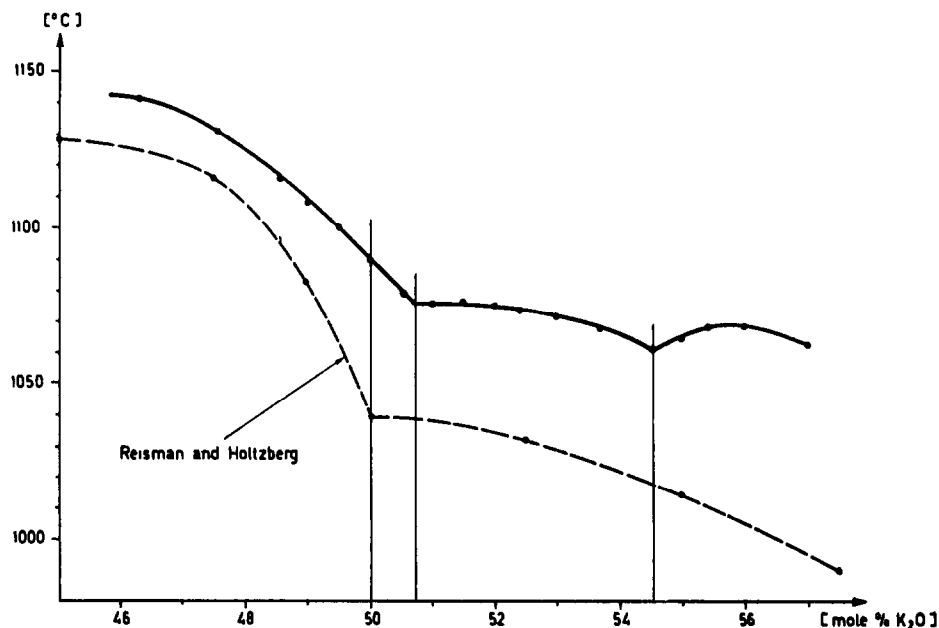


Fig. 5. Melting diagram for the system  $\text{Nb}_2\text{O}_5\text{-K}_2\text{O}$  near 50 mol%  $\text{K}_2\text{O}$  (—) Liquidus temperature, after Flückiger and Arend [30]. (---) Liquidus temperature, after Reisman and Holtzberg [29].

gruent melting, the peritectic and liquidus compositions being very similar. Inclusions of  $\text{KNd}(\text{MoO}_4)_2$  appeared in single crystals grown from stoichiometric melts, whereas a slight excess of  $\text{K}_2\text{MoO}_4$  in the melt caused inclusions of the eutectic in the crystals [34]. Similar results have been described for the  $\text{Rb}_2\text{MoO}_4\text{-Nd}_2(\text{MoO}_4)_3$  section. For comparison,  $\text{K}_5\text{Bi}(\text{MoO}_4)_4$  melts congruently [35]: it forms solid solutions  $\text{K}_5\text{Bi}_{1-x}\text{Nd}_x(\text{MoO}_4)_4$  for a wide range of  $x$  which can be easily grown as single crystals from the melt [33].

The DTA studies done by Turyanitsa et al. [36] revealed that the quasibinary system  $\text{SbI}_3\text{-Sb}_2\text{Te}_3$  contains one ternary compound ( $\text{SbTeI}$ ) which melts incongruently at  $T_p = 400^\circ\text{C}$ . The large difference between the peritectic and stoichiometric compositions and the high vapour pressure of the components suggest that gas-phase growth below  $T_p$  is preferred over growth from a rather non-stoichiometric melt containing a large excess of  $\text{SbI}_3$ .

#### SEARCH FOR THE EXACT COMPOSITION AT THE MELTING POINT MAXIMUM

Frequently experiences with the crystal growth of compounds reported to melt congruently cannot be explained satisfactorily on the basis of published phase diagrams. Therefore, more detailed studies of the melting behaviour are required in order to correct the phase relationships with respect to the

occurrence and range of solid solubilities or the non-stoichiometry of compounds. Crystal growth can then be attempted using as the starting mixture that composition which melts congruently. In this mixture both the temperatures and the compositions of the liquid and solid coincide, and temperature fluctuations during crystal growth should not influence the composition of the resulting solid. Consequently, crystals of improved homogeneity can be prepared. Fluctuations in physical (electrical and optical) properties which depend sensitively on the stoichiometry can be reduced or avoided.

There are three criteria which can be used to determine, from DTA traces, which concentration of a series melts congruently: (a) the disappearance of the eutectic effects; (b) the maximum of the melting temperature (liquidus temperature); and (c) the maximum of the melting enthalpy at the liquidus temperature. To allow definite conclusions to be drawn the samples must be well equilibrated prior to being subjected to DTA.

Method (a) derived by Offergeld and van Cakenberghe [37] holds for congruently melting phases with a narrow phase width, otherwise it indicates the phase width at either eutectic temperature. Lower melting eutectics appear on both sides of a congruently melting phase  $A_mB_n$  in the phase diagram of A-B. The eutectic effects become smaller the closer the approximation to the compound and disappear at the composition  $A_mB_n$ . From a plot of the magnitude (peak area or height) of the eutectic effect versus the composition (Fig. 6) the ratio  $m:n$  can be determined. In this way the congruently melting compositions of some binary semiconductor systems were found to be  $Sb_{40.4}Te_{59.6}$ ,  $Bi_{39.95}Te_{60.05}$  and  $Bi_{40.02}Se_{59.98}$ . For the system  $Bi_2O_3-P_2O_5$ , Schultze and Uecker [38] found, using this procedure, a congruently melting compound  $Bi_{5.80}PO_{11.20}$ , which could be pulled in single crystal form.

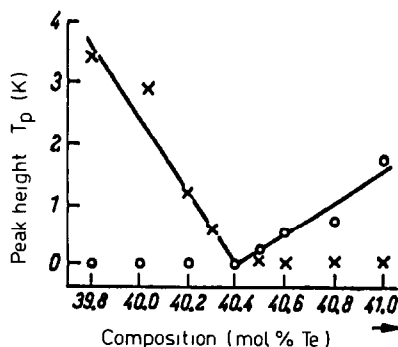


Fig 6 Determination of the congruently melting composition in the binary system Sb-Te peak heights of the DTA effect of the eutectics vs. composition. ( $\times$ ) Eutectic  $Sb_2Te_3-Te$ , ( $\circ$ ) eutectic  $Sb_2Te_3-Sb$ . Reprinted with the permission of Pergamon Press PLC from Offergeld and van Cakenberghe [37].

The appearance and magnitude of a eutectic effect give information about the purity of the crystals grown. Bohac and Kaufmann [39] monitored the purification of  $\text{Sb}_2\text{S}_3$  crystals by means of the zone refining technique, and Lazarev et al. [40] detected traces of arsenic in improperly prepared  $\text{CdAs}_2$  single crystals. Using the disappearance of the eutectic DTA effects, Gabrielian et al. [41] determined the phase width of  $\text{PbMoO}_4$  in the  $\text{PbO}-\text{MoO}_3$  system as 49.85–50.50 mol%  $\text{MoO}_3$ , which is in good agreement with results obtained using other techniques.

Method (c) can be applied to well-equilibrated samples if the enthalpy measurements are reproducible to within 0.1%. Thus this method is particularly useful preferably at temperatures below about  $700^\circ\text{C}$ , the maximum working temperature of quantitative DTA or DSC measurements.

Method (b) is the most generally applicable one for determining the congruently melting composition, even for systems with wide homogeneity ranges. All the phase diagram studies described in the following are based on this method of evaluating DTA measurements.

Reisman and Holtzberg [42] determined the phase diagram of  $\text{Li}_2\text{O}-\text{Nb}_2\text{O}_5$  by means of DTA, and found that  $\text{LiNbO}_3$  is a congruently melting compound. Single crystals grown from the melt were found to vary in terms of their Curie temperature, birefringence, and other properties. Elaborate DTA, X-ray diffraction and NMR studies revealed a solid solution range from 45 to 50 mol%  $\text{Li}_2\text{O}$  and a melting point maximum at 48.6 mol%  $\text{Li}_2\text{O}$  (Fig. 7) [43,44]. Melts of this composition are now used to grow “ $\text{LiNbO}_3$ ”

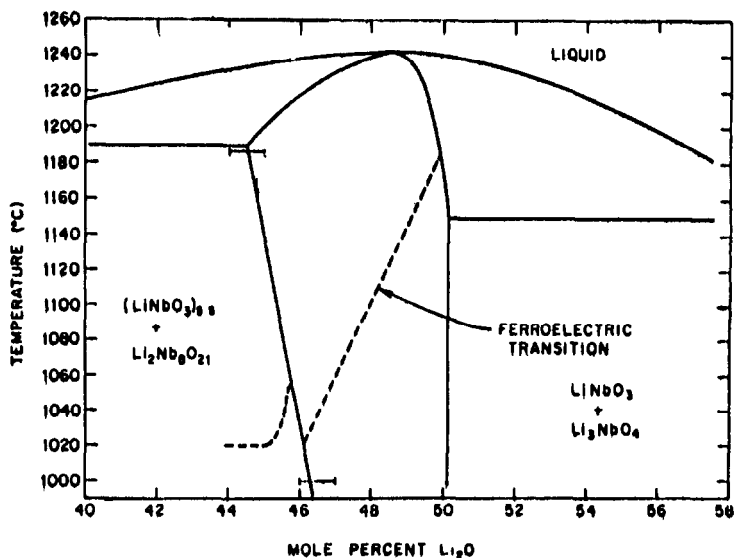


Fig 7 Equilibrium diagram of the  $\text{Li}_2\text{O}-\text{Nb}_2\text{O}_5$  system near 50 mol%  $\text{Li}_2\text{O}$  and ferroelectric transformation temperature vs composition Reprinted with the permission of The American Institute of Physics from Carruthers et al [44]

crystals of good homogeneity over their entire volume. Truly stoichiometric  $\text{LiNbO}_3$  crystals can be prepared from a melt containing an excess (58 mol%) of  $\text{Li}_2\text{O}$ ; however, high quality crystals cannot be expected to be obtained with the usual pulling technique under these conditions.

A congruently melting compound can be crystallized in the ternary system  $\text{SrO}-\text{BaO}-\text{Nb}_2\text{O}_5$ . DTA studies by Carruthers and Grasso [45] demonstrated the wide homogeneity range of this system which has its melting point maximum at the composition  $\text{Sr}_{0.46}\text{Ba}_{0.54}\text{Nb}_2\text{O}_6$ . Later DTA measurements by Megumi et al. [46] indicated a maximum melting temperature and a maximum degree of undercooling of the melt near the composition  $\text{Sr}_{0.6}\text{Ba}_{0.4}\text{Nb}_2\text{O}_6$ . The congruently melting composition was found at a slight deficit of  $\text{Nb}_2\text{O}_5$ , i.e.  $(\text{Sr}_{0.61}\text{Ba}_{0.39}\text{O})_{0.5007}(\text{Nb}_2\text{O}_5)_{0.4993}$ . Crystal growth experiments gave samples of improved homogeneity if this melt was used as the starting material.

DTA measurements along the quasibinary section  $\text{NaNbO}_3-\text{BaNb}_2\text{O}_6$  indicated extensive solid solubilities around a melting point maximum for  $\text{Ba}_2\text{NaNb}_5\text{O}_{15} = (\text{Ba}_{0.4}\text{Na}_{0.2}\text{O})_{0.5}(\text{Nb}_2\text{O}_5)_{0.5}$  [47]. Other investigations in which this system was considered as a ternary one resulted in congruently melting compositions deviating from the quasibinary section  $\text{BaNb}_2\text{O}_6-\text{NaNbO}_3$ , i.e.  $(\text{Ba}_{0.43}\text{Na}_{0.16}\text{O}_{0.51})(\text{Nb}_2\text{O}_5)_{0.49}$  [48] and  $(\text{Ba}_{0.422}\text{Na}_{0.144}\text{O}_{0.494})(\text{Nb}_2\text{O}_5)_{0.506}$  [49]. Exact determination of the liquidus surface of this ternary system is rather problematic because the liquidus surface is relatively flat and at that temperature ( $1455^\circ\text{C}$ ) the composition can alter due to the evaporation of  $\text{Na}_2\text{O}$ .

Using DTA along the quasibinary section  $\text{KNbO}_3-\text{Bi}(\text{NbO}_3)_3$ , Sugai and Wada [50] found the melting point maximum at  $\text{K}_2\text{BiNb}_5\text{O}_{15}$  which has a wide range of solid solubility. Crystal growth was started with this composition and resulted in a single crystal having the composition  $\text{K}_{1.5}\text{BiNb}_{5.1}\text{O}_{15}$ , suggesting that the congruently melting composition is situated on the niobium rich side of the quasibinary section in the ternary diagram. On further investigation of the ternary system  $\text{K}_2\text{O}-\text{Bi}_2\text{O}_3-\text{Nb}_2\text{O}_5$  and its Rb and Cs analogues, Sugai [51] found another type of compound, i.e.  $\text{MBi}_2\text{Nb}_5\text{O}_{16}$ . With  $\text{M} = \text{K}$  this compound melts incongruently, but for  $\text{M} = \text{Rb}$  or  $\text{Cs}$  congruently melting phases were detected and these crystals could be grown by means of the pulling technique.

Studies by Krämer et al. [52] on the  $\text{Ba}_2\text{O}-\text{Li}_2\text{O}-\text{Nb}_2\text{O}_5$  system have shown that  $\text{Ba}_2\text{LiNb}_5\text{O}_{15}$  melts incongruently. From a comparison of the sections  $\text{LiNbO}_3-\text{BaNb}_2\text{O}_6$  and  $\text{Li}_3\text{NbO}_4-\text{BaNb}_2\text{O}_6$ , investigated by DTA, the authors concluded that the latter is the preferred one from which to grow single crystals of  $\text{Ba}_2\text{LiNb}_5\text{O}_{15}$ , because the distance between the peritectic and stoichiometric compositions is narrower and the liquidus line is steeper than in the former section. The improved optical homogeneity of the single crystals obtained confirms this view.

The appearance of melting point maxima far from stoichiometric com-

TABLE 1

Systems of alkaline earth fluorides with rare earth fluorides that have been studied in relation to single crystal growth

System	RE	Concentration (mol% REF <sub>3</sub> )	Remarks <sup>a</sup>	Ref.
CaF <sub>2</sub> -GdF <sub>3</sub>		0-100		53
CaF <sub>2</sub> -YF <sub>3</sub> or NdF <sub>3</sub>		0-100	1	54
CaF <sub>2</sub> -REF <sub>3</sub>	La-Yb, Y	60-100	1	55
	La-Lu, Y	0-100	1	56
SrF <sub>2</sub> -REF <sub>3</sub>	La-Yb, Y	60-100	1	57
	La-Lu, Y	0-100	1	58
BaF <sub>2</sub> -REF <sub>3</sub>	La-Lu, Y	0-100	1, 2	18
CaF <sub>2</sub> -REOF	La, Gd, Y	0-100	3	59
SrF <sub>2</sub> -REOF				
BaF <sub>2</sub> -REOF				

<sup>a</sup> 1, Non-stoichiometric, congruently melting compounds are formed 2, With RE = Ho to Lu and Y, congruently melting BaRE<sub>2</sub>F<sub>8</sub> are formed. 3, Solid solutions of wide homogeneity are formed, single crystals up to 10% REF<sub>3</sub> are grown

positions in systems of alkaline earth and rare earth fluorides, which are potential laser systems, prompted extensive investigation into their phase diagrams. Thorough DTA studies done by Sobolev, Fedorov and others [53-59] clarified the phase relationships and became the basis of successful growth experiments (Table 1). Non-stoichiometry of congruently melting compositions is a common phenomenon in ternary chalcogenide systems. In the quasibinary sections Tl<sub>2</sub>S-GeS<sub>2</sub> and Tl<sub>2</sub>Se-GeSe<sub>2</sub> Peresh et al. [60] found the liquidus maxima to occur not exactly at Tl<sub>4</sub>GeS<sub>4</sub> or Tl<sub>4</sub>GeSe<sub>4</sub> but at slightly GeS<sub>2</sub> or GeSe<sub>2</sub> deficient compositions. Crystals having uniform composition along their length can be grown from such off-stoichiometric melts. DTA measurements on the concentration dependence of the eutectic effects enabled the limits of the solid solubilities to be determined. In contrast to these thio- and seleno-germanates, the analogous thio- and seleno-stannates Tl<sub>2</sub>SnS<sub>3</sub>, Tl<sub>2</sub>SnSe<sub>3</sub>, Tl<sub>4</sub>SnS<sub>4</sub> and Tl<sub>4</sub>SnSe<sub>4</sub> do melt congruently at their stoichiometric compositions and can be grown as single crystals of these formulae [61].

Especially with sulphides and selenides, DTA studies of phase diagrams suffer additional complications due to partial evaporation of one component, even if hermetically sealed ampoules are used as sample containers. Evaporation can be reduced by minimizing the gas space above the sample and by adjusting the temperature gradient such that the top of the ampoule is hotter than the lower part, thus preventing transport of the volatile component out of the melt. If the vapour pressure of the most volatile compound is known, the composition of the condensed phase for the maximum loss of this component at a particular temperature can be calculated. In this way Nelson et al. [62] have corrected the melt compositions of

the system HgSe–CdSe for the selective evaporation of mercury into the gas space of the ampoule. Liquidus and solidus temperatures determined by DTA were then assigned to the corrected composition data. The same procedure has been applied by Szofran & Lehoczky [63] in studies of the Cd–Hg–Te ternary system.

In the quasibinary section  $\text{Ag}_2\text{Se}-\text{Ga}_2\text{Se}_3$  of the ternary Ag–Ga–Se, Route et al. [64] found, by DTA, a melting point maximum at the composition  $\text{AgGaSe}_3$ . Along the AgGa–Se section a maximum was also found for this composition, confirming the congruent melting of this compound. However, complicated multi-phase relationships occur in slightly selenium deficient compositions. Therefore, crystal growth experiments must start from a stoichiometric melt and selenium evaporation must be strictly avoided in order to achieve crystals of sufficient quality. A reinvestigation of the quasibinary  $\text{Ag}_2\text{Se}-\text{Ga}_2\text{Se}_3$  system by Mikkelsen [65] has confirmed the congruent melting of  $\text{AgGaSe}_2$ , but established the formation of solid solutions of  $\text{Ga}_2\text{Se}_3$  in  $\text{AgGaSe}_2$ . The solid solubility is retrograde and leads to precipitation of a  $\text{Ga}_2\text{Se}_3$  related phase when single crystals are cooled. Furthermore, another compound ( $\text{Ag}_9\text{GaSe}_6$ ) was also discovered in the quasibinary section  $\text{Ag}_2\text{Se}-\text{Ga}_2\text{Se}_3$ .

In a study to determine the conditions required to grow  $\text{CuGaS}_2$  crystals, Kokta et al. [66] evaluated, by means of DTA, various sections of the Cu–Ga–S ternary system. The results suggest a melting point maximum at the non-stoichiometric composition  $\text{Cu}_{0.225}\text{Ga}_{0.245}\text{S}_{0.530}$ , i.e. a composition containing a remarkable excess of gallium and sulphur. Crystals grown from this composition, however, did not show the luminescence properties of the stoichiometric material. In accordance with the phase diagram, stoichiometric crystals must be grown from melts having a Cu:Ga ratio of 1 and an excess of sulphur, and with the usual precautions taken when growing non-congruently melting compounds.

The only ternary compound in the Cu–Ga–Se system is the incongruently melting chalcopyrite phase ( $\text{CuGaSe}_2$ ) with a phase width of 50–58%  $\text{Ga}_2\text{Se}_3$  [67]. Furthermore, solid solutions based on  $\text{Ga}_2\text{Se}_3$  and having a maximum melting point at  $\text{Cu}_{19}\text{Ga}_{285}\text{Se}_{525}$  are present in the quasibinary section  $\text{Cu}_2\text{Se}-\text{Ga}_2\text{Se}_3$ . The narrow interval between the peritectic melting temperature of  $\text{CuGaSe}_2$  ( $1030^\circ\text{C}$ ) and its eutectic with  $\text{CuSe}_2$  ( $970^\circ\text{C}$ ) suggest that, for single crystal growth of  $\text{CuGaSe}_2$ , crystallization by zone melting is preferred over Bridgman growth from the off-stoichiometric melt.

Using DTA, Binsma et al. [68] found two congruently melting compounds in the  $\text{Cu}_2\text{S}-\text{In}_2\text{S}_3$  quasibinary section:  $\text{CuInS}_2$  underlies two phase transformations which prevent single crystals grown from the stoichiometric melt from surviving cooling to room temperature. Verheijen et al. [69] assume that the thermal effects seen below the liquidus temperature in  $\text{CuInS}_2$  are due to an eutectic and to a solid–solid transition. The common consequence of these two contradictory interpretations is that single crystals of  $\text{CuInS}_2$

should not be grown from stoichiometric melts but perhaps from a solution in a metal (In or Cu–In alloy) or by gas transport. Single crystals of solid solutions of the pseudobinary system  $\text{CuInSe}_{2x}\text{S}_{2(1-x)}$  prepared by gas transport exhibit two solid–solid transformations if  $x = 0.3$  or  $x = 0.7$ ; this result confirms the interpretation proposed by Binsma et al. [68]. Single crystals were deposited at a temperature below the lowest polymorphic transformation [70].

A phase diagram study of the As–Te system [71] revealed congruently melting  $\text{As}_2\text{Te}_3$  as the only binary compound; it crystallizes only at significant undercooling. Then, after initiation of the nucleation, the crystallization proceeds very rapidly and is strongly anisotropic. To avoid fibrous crystallization and to prepare crystal boules containing a few large single crystalline grains, a Bridgman technique is employed which combines a steep vertical gradient with a flat horizontal temperature gradient and an ampoule with a narrow neck above the nucleation room at the bottom of the ampoule.

According to Krämer [72], the DTA of samples in sulphide systems pre-reacted by sintering processes does not necessarily provide data on all the phases present in the system under study, because subsolidus equilibria are established very slowly. Chemical vapour transport studies can provide additional information, either to support or to complement the DTA data. New phases prepared by gas transport reactions can then again be subjected to DTA in order to study their melting behaviour and to improve the melting diagram. Transport experiments have shown that two ternary phases exist in the  $\text{PbS–In}_2\text{S}_3$  system near the 1:1 molar ratio, in contrast to the previously accepted melting diagram which shows only one ternary phase ( $\text{PbIn}_2\text{S}_4$ ). DTA measurements made at slow heating rates ( $2 \text{ K min}^{-1}$ ) to overcome kinetic barriers [73] have confirmed the existence of the second compound ( $\text{Pb}_9\text{In}_{20}\text{S}_{39}$ ) and the congruent melting. In the  $\text{Bi}_2\text{S}_3\text{–In}_2\text{S}_3$  quasibinary section, Krämer [74] found, by DTA, three modifications of  $\text{In}_2\text{S}_3$  and only one ternary compound ( $\text{In}_2\text{Bi}_4\text{S}_9$ ), whereas chemical vapour transport enabled the preparation of two more compounds,  $\text{InBiS}_3$  and  $\text{In}_4\text{Bi}_2\text{S}_9$ , the existence of which was confirmed by means of DTA of mixtures of the elements that had been annealed for an extremely long time.

The travelling solvent technique of crystal growth delivers a series of samples along one ingot, each sample having its equilibrium solidus composition at its particular crystallization temperature. Chemical analysis of these samples together with DTA measurements allow the exact solidus temperature of equilibrated samples to be determined. Using this method Strassburger [75] constructed the phase diagram Bi–Te. The phase width of congruently melting  $\text{Bi}_2\text{Te}_3$  was found to be at  $\text{Bi}_{39.78-40.17}\text{Te}_{60.22-59.83}$ . Another incongruently melting compound with a rather large phase width was confirmed to crystallize between 46 and 58 at% Bi. This method of phase diagram evaluation is advantageous as it does not require time-consuming annealing procedures of separate samples to achieve equilibrium.

However, the composition of each sample taken from the ingot must be determined independently.

#### CRYSTALLIZATION OF METASTABLE PHASES

If a solid is frozen from the melt the crystallizing phase will not necessarily be the 'stable' one having the lowest free enthalpy. According to the Ostwald step rule, another solid phase can be formed first. The transformation to the stable solid phase may occur after some delay and with a substantial undercooling. Such a solid–solid transformation will affect or disturb the previously grown single crystals. DTA measurements and a comparison of heating and cooling curves obtained for samples of different thermal pretreatment can help in differentiating between the stable and metastable phase relationships.

The  $\text{Gd}_2\text{O}_3\text{--Ga}_2\text{O}_3$  system contains two congruently melting compounds  $\text{GdGaO}_3$  (perovskite) and  $\text{Gd}_3\text{Ga}_5\text{O}_{12}$  (garnet), the melting point maximum of the latter occurring at a somewhat deviating composition  $\text{Gd}_{3.05}\text{Ga}_{4.95}\text{O}_{12}$  [76]. Melts of the latter composition crystallize with extensive undercooling [77] either after heating to a maximum temperature of 20 K above the melting point, yielding garnet, or after superheating to more than 20 K above the melting point, yielding a mixture of perovskite and  $\text{Ga}_2\text{O}_3$ . DTA cooling curves show one exotherm for the first case and two exotherms for the second. Upon reheating the two-phase mixture, DiGiuseppe et al. [78] found a series of endothermic DTA effects (Fig. 8). The sample starts to melt far below the eutectic temperature in the stable phase diagram and then a reaction or dissolution of the remaining solid occurs. Alternatively, the effects may indicate the exothermic reformation of the garnet phase by reactions in the mixture followed by melting at the stable melting temperature. These results may be explained by a metastable extension of the stable liquidus curves in the melting diagram  $\text{Gd}_2\text{O}_3\text{--Ga}_2\text{O}_3$  down to a metastable eutectic between  $\text{GdGaO}_3$  and  $\text{Ga}_2\text{O}_3$ . Obviously the melt transforms from a garnet-like structure to some other structure when heated to above a critical temperature, this transformation not being readily reversible. The crystallization of the garnet phase from the superheated melt will, therefore, have a higher activation energy than that of the perovskite phase. This idea has been confirmed by the results obtained from DTA experiments at different cooling rates  $\bar{\beta}$ , where the perovskite crystallization exotherm was broadened at small  $\bar{\beta}$ , whilst that of the garnet crystallization was unaffected. Similar results were obtained for the  $\text{Sm}_2\text{O}_3\text{--Ga}_2\text{O}_3$  system.

The crystallization of yttrium aluminium garnet ( $\text{Y}_3\text{Al}_5\text{O}_{12}$ ) from its melt shows the same phenomenon. Using a DTA system with pyrometric temperature sensors, Caslavsky and Viechnicki [79] established both a stable and a metastable melting diagram for the  $\text{Al}_2\text{O}_3\text{--YAlO}_3$  section, depending on the degree of superheating of the melt. Presumably a change in the coordination

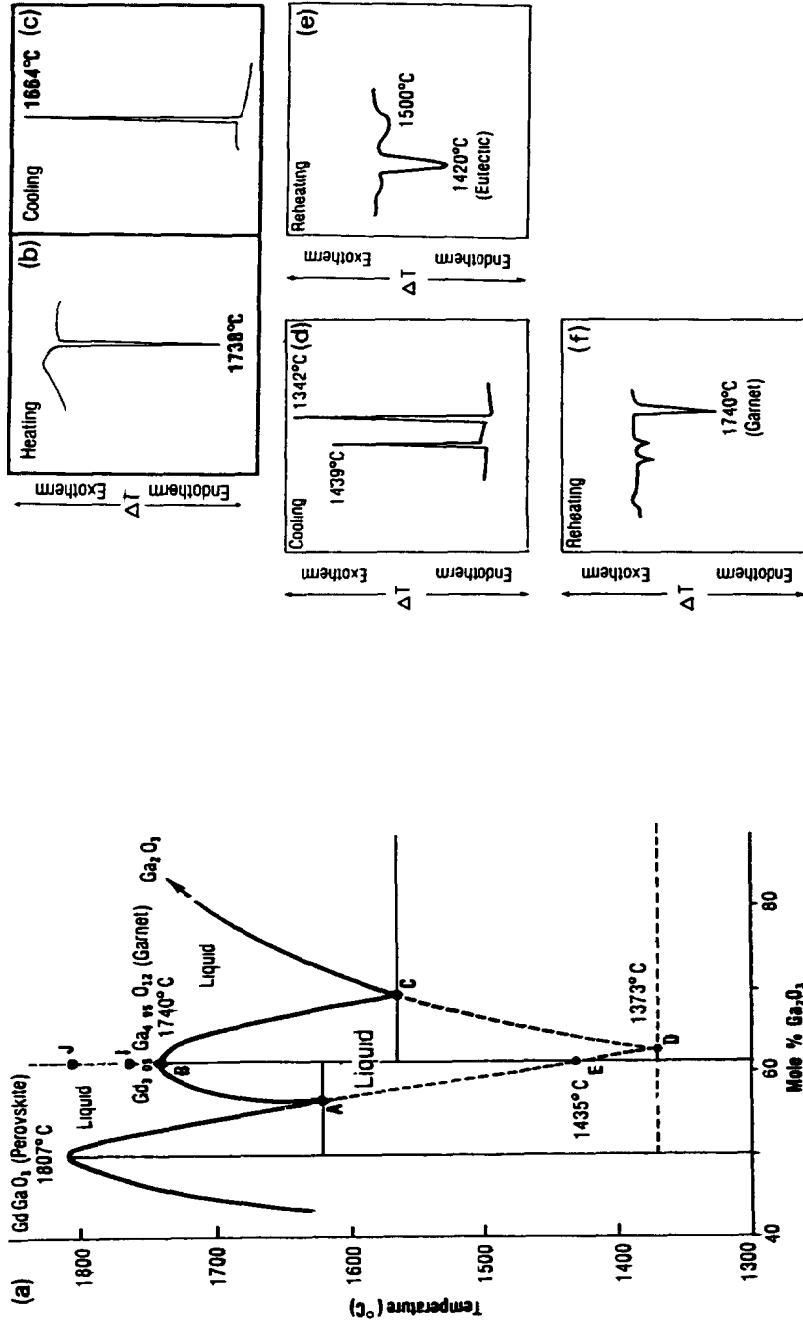


Fig. 8. DTA studies on the  $Gd_2O_3-Ga_2O_3$  system. (a) stable (—) and metastable (---) liquidus curves and the corresponding eutectic horizontal. (b) Heating curve of the melt after heating to  $1755^\circ C$ . (c) Cooling curve of the metastable eutectic followed by dissolution of the excess garnet phase. (d) Cooling curve showing melting of the metastable eutectic followed by melting of the residual eutectics and the melting of the garnet phase. (e) Reheating curve showing solid state reaction to the garnet phase followed by melting of the residual eutectics and the melting of the garnet phase. Reprinted with the permission of Academic Press from DiGruseppe et al. [78] ((a), (e) and (f)) and DiGruseppe and Soled [77] ((b), (c) and (d)).

of the  $O^{2-}$  ions surrounding the  $Al^{3+}$  cation in the melt is the reason for this behaviour. To exclude any affect on single crystal growth experiments excessive superheating of garnet melts must be avoided.

A similar sensitivity towards superheating has been detected by DTA and crystallization experiments of the CdSb phase from a stoichiometric alloy [80]. In this case, however, partial evaporation of cadmium from the melt cannot be excluded and different melt compositions having different crystallization properties are obtained.

Vast regions of metastable crystallization have been found in the  $Bi_2O_3$ - $GeO_2$  system. There are three stable compounds, namely  $Bi_{12}GeO_{20}$  (I),  $Bi_4Ge_3O_{12}$  (II), and  $Bi_2Ge_3O_9$  (III), all of which have been pulled as single crystals from their respective melts, but with unsatisfactory results and poor reproducibility. The contradictory results concerning the phase diagram and the crystallization behaviour obtained by other workers led to a reinvestigation of the melting diagram [81], mainly by means of the DTA technique. The stable phase diagram showed that compounds I and II melt congruently and III incongruently, with eutectic horizontals (A) between  $Bi_2O_3$  and I, (B) between I and II, and (C) between III and  $GeO_2$ . The liquidus lines  $Bi_2O_3$ -A and C- $GeO_2$  extend metastably to form lower melting eutectics of  $Bi_4Ge_3O_{12}$  with  $GeO_2$  and  $Bi_2O_3$  or a  $\delta$ - $Bi_2O_3$  like phase. In addition, there is a metastable diagram which is governed by the compound  $Bi_2GeO_5$  (IV). This compound forms metastable eutectics with both  $GeO_2$  and the  $\delta$ - $Bi_2O_3$  phase.

The stable system was evaluated using the DTA heating curves of the respective mixtures of the stable compounds. The melts thus obtained can be supercooled and, upon freezing, the metastable compound ( $Bi_2GeO_5$ ) crystallized (plus either  $GeO_2$  or  $Bi_2O_3$ ). Depending on the further treatment (annealing, further cooling or immediate reheating) the metastable phase more or less transforms to the stable ones. Consequently, the DTA curves recorded during the second heating run depend strongly on the thermal history of the sample. The striking trend to freezing in the metastable system may be due to the fact that the structure of the melt is closely related to that of  $Bi_2GeO_5$  but not to  $Bi_4Ge_3O_{12}$ , so that the former is more easily nucleated. Therefore, to grow  $Bi_4Ge_3O_{12}$  single crystals one must use a seed of this latter compound and carefully exclude possible supercooling of the melt by imposing a steep temperature gradient at the grownig interface.

The phase diagram for the  $PbO$ - $GeO_2$  system has been the subject of controversy. Even the more recent studies [82,83] do not agree totally. Melting point maxima were consistently found for the compositions  $PbGeO_3$ ,  $Pb_5Ge_3O_{11}$ , and  $Pb_3GeO_5$ . Various other compositions were proposed for incongruently melting or metastable compounds. Here DTA investigations reach their limits of application, because phase equilibria are established slowly and metastable phases can crystallize more rapidly than the stable ones from supercooled melts or heated glasses. An alternative method,

“sol-gel”, for preparing more reactive homogeneous material is based on the simultaneous hydrolysis of lead and germanium alkoxides followed by thermal dehydration. The large specific surface of the amorphous products obtained in this way facilitates their crystallization. The heating of such materials yielded  $\text{Pb}_5\text{Ge}_3\text{O}_{11}$  and  $\text{PbGeO}_3$ , primarily in modifications different from the known ones [84]. Upon further heating to higher temperatures these compounds transformed exothermically to the known modifications. These transformations and the melting of the respective compounds may be monitored by means of DTA. No indication of the questionable compound  $\text{Pb}_3\text{Ge}_2\text{O}_7$  was found in this way. This alkoxide procedure cannot be presumed necessarily to circumvent all kinetic hindrances towards the establishment of equilibrium within the time interval of a DTA experiment. In very slowly equilibrating systems, quenching samples that have been annealed for a long time, followed by X-ray diffraction and microscopic investigations appears more appropriate.

#### CRYSTALLIZATION FROM HIGH TEMPERATURE SOLUTIONS (FLUXES)

High temperature solutions (fluxes) are used to grow single crystals of materials that cannot be prepared directly from their melt, due to modification changes, peritectic decomposition, or gas evolution at a certain temperature ( $T_i$ ) between ambient and liquidus temperature ( $T_l$ ). In these cases the liquidus temperature must be depressed below  $T_i$  by adding a sufficient amount of the flux. Upon cooling to below the liquidus temperature the solution becomes supersaturated and the solute crystallizes.

In relation to crystal growth from high temperature solutions, DTA phase diagram studies provide information about; (i) the minimum amount of solvent required to achieve  $T_l < T_i$ , i.e. the maximum temperature required for the growth process; (ii) the eutectic temperature ( $T_e$ ), i.e. the minimum temperature required for the growth process; and (iii) the solubility curve  $x$  vs.  $T_l$  between  $T_i$  and  $T_e$ . Furthermore, comparison of DTA heating and cooling curves allows conclusions to be drawn about the ability of the solution to undercool before crystallization commences. Thus the width of the metastable region between the equilibrium liquidus and spontaneous nucleation can be estimated.

If high temperature solutions are to be studied by means of DTA some particular problems must be solved. (i) If the liquidus temperature increases relatively rapidly with  $x$ , as is usually the case, the thermal effect is flattened and broadened over a wide temperature interval, rendering the determination of  $T_l$  difficult. Therefore, a high-sensitivity DTA measuring head (not a block system), carefully shielded against parasitic voltages, a non-inductively wound furnace and an appropriate controller for minimizing temperature fluctuation are essential. (ii) The difference in the densities of the solute and the solvent results in a concentration of solids before dissolution either near

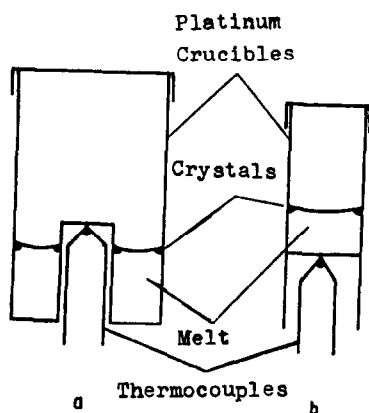


Fig. 9 Possible positions of the DTA thermocouple relative to the last-to-dissolve particles (a) Advantageous for  $\rho_{\text{melt}} > \rho_{\text{crystals}}$  (b) Advantageous for  $\rho_{\text{crystals}} > \rho_{\text{melt}}$  Reprinted with the permission of Akademie-Verlag GmbH from Fischer [87]

the bottom or the surface of the sample. The DTA thermocouple should be positioned as near as possible to the area where the last particles dissolve. Figure 9 shows the situation where the melt is more dense than the crystals. Here a sample holder of the design shown in Fig. 9(a) is preferred. DTA apparatus for liquidus measurements of high-temperature solutions have been described elsewhere [85–87]. (iii) As many high temperature solutions exhibit a remarkable tendency to undercool, DTA heating curves are favoured over cooling curves for determining  $T_1$ . It is virtually impossible to nucleate the freezing of a cooling melt in the DTA system by adding small crystallites from outside without causing severe disturbance of the thermal conditions inside. Sometimes heterogeneous nucleation by insoluble particles (e.g. Pt for oxidic melts or quartz for chalcogenides or pnictides) reduces or prevents undercooling to some extent. However, the abrupt onset of crystallization in an undercooled melt is more easily recognized on a DTA cooling curve than is the end of dissolution on a DTA heating curve. From DTA curves recorded at various cooling rates,  $\bar{\beta}$ , one can extrapolate to  $\bar{\beta} = 0$  and thus estimate the equilibrium liquidus temperature. Furthermore, in a melt rapidly cooled from a temperature  $> T_1$  to a certain temperature between the liquidus and eutectic temperatures and then held isothermally, crystallization occurs after a certain time interval,  $t_i$ , which can be measured using DTA. The dependence of this induction time,  $t_i$ , on the thermal pretreatment, e.g. soaking at various temperatures above or below the liquidus temperature, allows conclusions to be drawn about the nucleation mechanism [88–90].

When growing crystals using the high temperature solution technique, solvents having one component in common with the solute are preferred. For example, to prepare GaAs or GaP crystals, metallic gallium is an appropriate solvent. There is a gradual transition between crystallization

from non-stoichiometric melts (at lower solvent concentration) to crystallization from high temperature solution (at lower solute concentration).

The literature data for the liquidus temperatures and thermodynamic properties of the systems Ga–GaP and In–InP vary widely due to the experimental difficulties involved with the use of high phosphorus pressure. In a critical review of results obtained with DTA and other techniques, Tmar et al. [91] derived optimized phase diagrams consistent with sets of thermodynamic data. It can be concluded that DTA is a suitable technique for studying these systems and for obtaining results of a quality comparable to those obtained with other techniques. A DTA study by Imai et al. [92] of the binary system In–Se at 30–60 at% Se proved the existence of three incongruently melting compounds, i.e.  $\text{In}_4\text{Se}_3$ , InSe and  $\text{In}_6\text{Se}_7$ . To improve the yield and quality of InSe monocrystals obtained by the Bridgman technique, the starting composition was taken as one close to the peritectic point of InSe, in this case with a slight excess of In.

The PbS–CdS system has been investigated using DTA by Olejnik et al. [93]. This system is eutectic with a high solubility of CdS in solid PbS and a very limited solid solubility of PbS in CdS. From the melting diagram suitable conditions for growing Pb doped CdS crystals were derived: the travelling heater method with PbS as solvent. In the pseudoternary system CdS–CdSe– $\text{CdCl}_2$ , solid solutions of composition  $\text{CdS}_{1-x}\text{Se}_x$  can be grown from  $\text{CdCl}_2$  solvent, for a wide range of  $x$ ; this was concluded from an evaluation of the liquidus temperatures measured by means of DTA [94].

The solubility of a material in a complex solvent is affected by the concentration of the solvent components. In an early DTA study, Elwell et al. [85] demonstrated that the liquidus temperature of solutions of  $\text{NiFe}_2\text{O}_4$  in  $\text{BaO} \cdot x\text{B}_2\text{O}_3$  melts decrease with increasing  $x$  ( $x = 0.5\text{--}1.0$ ). More recently, Eigermann et al. [95] found that the addition of PbO to  $\text{REPO}_4\text{--Pb}_2\text{P}_2\text{O}_7$  melt solutions decreased the liquidus temperature and improved the crystal growth of  $\text{YPO}_4$  and other  $\text{REPO}_4$ . Similarly, the addition of  $\text{Na}_2\text{B}_4\text{O}_7$  to the  $\text{NaVO}_3$  solvent enhanced the solubility of  $\text{YVO}_4$ . Fischer [87] used DTA to study the influence of the solvent compositions  $(\text{PbO})_{49.1\text{--}55} \cdot (\text{PbF}_2)_{36.5\text{--}42} \cdot (\text{B}_2\text{O}_3)_{4.1\text{--}14.5}$  on the liquidus temperature of  $\text{Gd}_3\text{Ga}_5\text{O}_{12}$  solutions.

The crystallization of ferroelectric  $\text{PbNb}_2\text{O}_6$  (tetragonal) from fluxes in the  $\text{PbO--Nb}_2\text{O}_5\text{--B}_2\text{O}_3$  system is complicated by the occurrence of other lead niobates and paraelectric (rhombohedral)  $\text{PbNb}_2\text{O}_6$ . Sholokhovich and Dugin [96] used DTA and other techniques to measure liquidus temperatures and to optimize the conditions for the growth of tetragonal  $\text{PbNb}_2\text{O}_6$ .

The DTA heating and cooling curves of  $\text{CsLa}(\text{WO}_4)_2$  led Ivannikova et al. [97] to conclude that this compound melts incongruently but with the simultaneous, or successive, formation of two solids, i.e.  $\text{La}_2(\text{WO}_4)_3$  and  $\text{La}_2\text{W}_2\text{O}_9$ . A detailed DTA investigation of the ternary reciprocal field  $\text{Cs}_2(\text{WO}_4)\text{--Cs}_2\text{W}_2\text{O}_7\text{--La}_2(\text{WO}_4)_3\text{--La}_2\text{W}_2\text{O}_9$  clearly showed that  $\text{CsLa}$ –

$(\text{WO}_4)_2$  should preferably be grown from a high temperature solution in  $\text{Cs}_2\text{W}_2\text{O}_7$ .

Crystallization from fluxes is of technical importance in the liquid phase epitactic (LPE) deposition of thin monocrystalline layers. This procedure must be carried out in the temperature and concentration interval between the equilibrium liquidus and the spontaneous nucleation curves. Both can be determined from DTA heating and cooling curves, respectively, as demonstrated by Baudrant et al. [98] (Fig. 10(a)) for the quasibinary system  $\text{LiNbO}_3(\text{solute})\text{-LiVO}_3(\text{solvent})$ . The liquidus data (curve 1) were obtained from the end of the dissolution endotherm on the DTA heating curve at a heating rate of  $\beta = 5$  or  $10 \text{ K min}^{-1}$  for various  $\text{LiNbO}_3:\text{LiVO}_3$  ratios. Unfortunately this effect becomes barely discernible at low solute concentrations, so the DTA measurements had to be complemented by other techniques (gravimetry and microscopic measurements) to construct curve 1. DTA studies of the same samples at constant cooling rates showed exothermal effects upon spontaneous nucleation and crystallization of the  $\text{LiNbO}_3$  phase at lower temperatures than curve 1. A plot against the concentration of  $\text{LiNbO}_3$  yielded the critical nucleation curve (curve 2). The crystallization temperature depends on the cooling rate,  $\bar{\beta}$ , as shown later by Hemmerling et al. [99] (Fig. 10(b)), and an extrapolation to  $\bar{\beta} = 0$  yielded the liquidus temperatures, again in reasonable agreement with those of Baudrant et al. [98]. Somewhat deviating results on the liquidus temperatures of this system have been obtained from DTA measurements by other workers [100,101].

The solubility of substituted lithium niobate, e.g.  $\text{Li}_{1-x}\text{Na}_x\text{NbO}_3$  ( $x = 0$  to  $0.15$ ) or  $\text{Li}_{1-x}\text{Co}_x\text{Nb}_{1-x}\text{Zr}_x\text{O}_3$ , in  $\text{LiVO}_3$  showed no change against that of pure  $\text{LiNbO}_3$  [102]. However,  $\text{LiVO}_3\text{-LiNb}_{1-x}\text{Ta}_x\text{O}_3$  ( $x = 0$  to  $1$ ) sections revealed at increasing  $x$  a continuous shift of liquidus curves to higher temperatures and increasing steepness of liquidus lines [103,104] (Fig. 10(c)). Here the liquidus temperatures were measured at relatively high heating rates ( $\beta = 20 \text{ K min}^{-1}$ ) and these curves should not be compared with those shown in Figs. 10(a) and 10(b). However, as expected, the results suggest that thin films of solid solutions at all  $x$  can be prepared by LPE deposition.

The crystallization of iron containing epitaxial garnet layers e.g.  $\text{Y}_3\text{Fe}_5\text{O}_{12}$ , from lead containing melts is more complicated due to the tendency to precipitation of  $\text{YFeO}_3$  and  $\text{PbFe}_{12}\text{O}_{19}$ . Therefore the system cannot be treated as a quasibinary one (solvent-solute). Jonker [105] has used DTA to measure liquidus temperatures of the partial system  $\text{PbO} \cdot n\text{B}_2\text{O}_3\text{-Fe}_2\text{O}_3$  ( $n = 0$  to  $0.2$ ). The solubilities of  $\text{Y}_3\text{Fe}_5\text{O}_{12}$  in a  $\text{PbO}(36.7 \text{ mol}\%)\text{-PbF}_2(27.3)\text{-B}_2\text{O}_3(5.4)\text{-Fe}_2\text{O}_3(3.4)$  melt have been determined by Görnert and D'Ambly [106] from DTA and gravimetric investigations. The solubilities of related garnet solid solutions  $\text{Y}_3\text{Fe}_{5-x}\text{Ga}_x\text{O}_{12}$  ( $x = 0\text{-}5$ ),  $\text{Y}_3\text{Al}_5\text{O}_{12}$ ,  $\text{Y}_3\text{Fe}_4\text{CrO}_{12}$  and  $\text{Y}_3\text{Fe}_4\text{InO}_{12}$  have been determined by Fischer [87]. Cryoscopic DTA investigations by Fischer [107,108] confirmed that the garnet

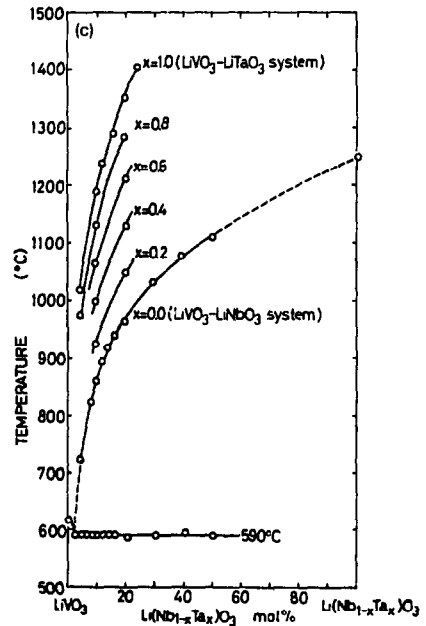
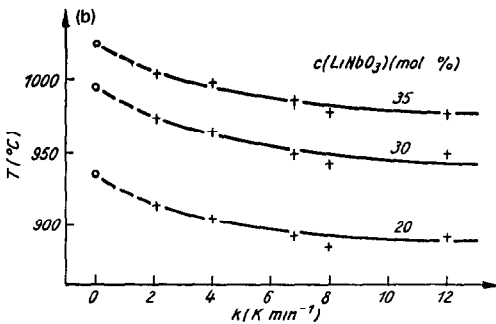
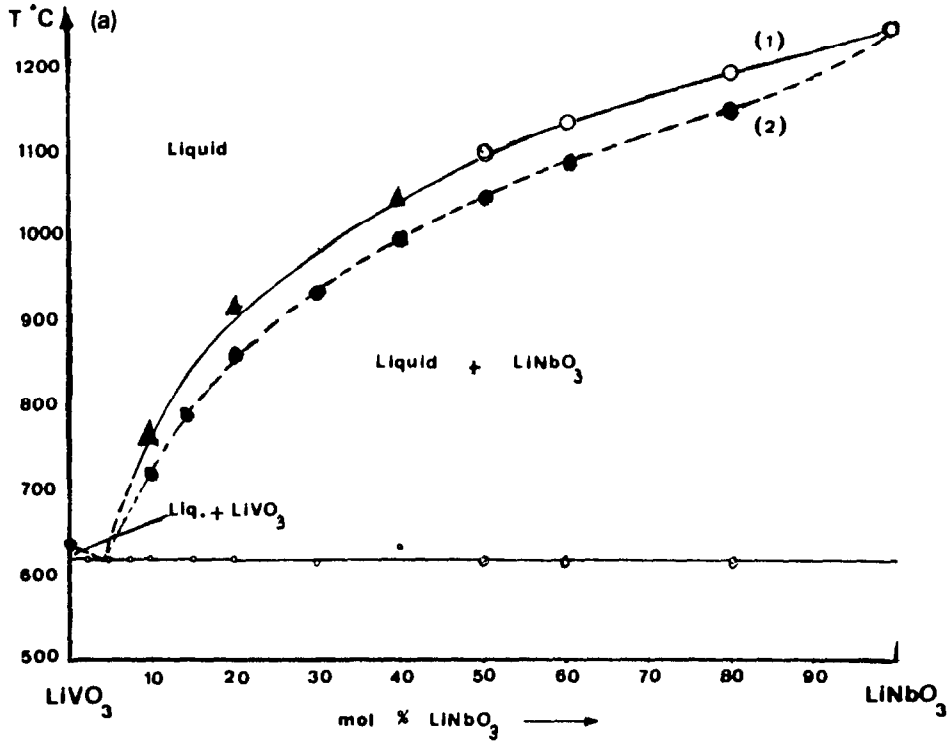


Fig. 10 DTA investigations on the  $\text{LiVO}_3$ - $\text{LiNbO}_3$ - $\text{LiTaO}_3$  system. (a) Liquidus (1) and critical nucleation (2) curves of the quasibinary section  $\text{LiVO}_3$ - $\text{LiNbO}_3$ . Reprinted with the permission of Pergamon Press PLC from Baudrant et al. [98]. (b) Dependence of (+) the nucleation temperature of solutions of  $\text{LiNbO}_3$  in  $\text{LiVO}_3$  on the cooling rate, and (○) extrapolation to a cooling rate of  $\beta = 0$ . Reprinted with the permission of Akademie-Verlag from Hemmerling et al. [99]. (c) Liquidus curves of quasibinary sections  $\text{LiVO}_3$ - $\text{LiNb}_{1-x}\text{Ta}_x\text{O}_3$ . From Kondo et al. [104].

dissolves in PbO with complete dissociation (eight particles per formula unit).

DTA studies of the CdTe–CdCl<sub>2</sub> system showed that CdCl<sub>2</sub> is a suitable solvent for growing CdTe layers by LPE deposition [109]. Similarly, Sashital [110,111] found that layers of AgGaS<sub>2</sub> (pure or doped with Ge) can be grown from a solution in molten KCl at temperatures where no interaction with the substrate (pure AgGaS<sub>2</sub>) occurs. DTA measurements along the isopleth 3AgGaS<sub>2</sub> · Ge–KCl of the quasiternary phase diagram gave proper concentration and temperature data for the liquid phase epitaxial process.

Layers of A(III)B(V) compounds, either as binary compounds or as solid solutions with or without heterovalent dopants, have found increasing application in electronics. Phase diagram studies as a basis for LPE deposition crystallization work have been carried out by many workers (see Table 2).

To reduce the amount of experimental work required, liquidus temperatures can be calculated from known thermodynamic data (entropy and temperature of melting of pure binary compounds) and activity coefficients of the components by using the “regular solution” model. The activity coefficients are derived by fitting the experimental liquidus and solidus data measured by DTA of selected compositions [112]. The methods of calculations have been reviewed by Kühn and Leonhardt [113].

The recent discovery of and widespread research on new “high-temperature” superconductors have prompted the investigation of the single crystal growth of these complex oxide materials. All oxide superconductors known so far melt incongruently and exhibit complicated phase relationships including oxygen non-stoichiometry. Therefore, simultaneous TG–DTA studies under a controlled atmosphere can be used to elucidate the phase diagrams. Further problems arise from the reactivity of alkaline earth oxide–copper oxide melts towards platinum or alumina crucibles and the tendency of partially molten samples to creep out of the crucible. Changes occur in the composition of the sample, resulting in impurities. Consequently, only the data obtained from the first heating over the super-solidus region can be accepted as reliable. Careful sample preparation by repeated grinding, pressing and sintering or the use of advanced synthetic techniques (joint precipitation or sol–gel preparation) helps thermal equilibrium to be reached before the DTA measurement is made.

DTA measurements in the La<sub>2</sub>O<sub>3</sub>–CuO, Nd<sub>2</sub>O<sub>3</sub>–CuO binary sections and their modification by doping with SrO or BaO were the basis for experiments done on crystal growth of superconducting (La,Ba)<sub>2</sub>CuO<sub>4</sub> [114,115], (La,Sr)<sub>2</sub>CuO<sub>4</sub> [116] and (Nd,Ce)<sub>2</sub>CuO<sub>4</sub> [117]. Many investigations were concerned with YBa<sub>2</sub>Cu<sub>3</sub>O<sub>7–x</sub> (“123”). Problems associated with the crystal growth and thermal analysis of this system have been reviewed [118]. This compound melts incongruently with a loss of oxygen at 1020 °C in air or 1050 °C in oxygen. Therefore, crystal growth is only possible from fluxes

TABLE 2

Systems containing high temperature solutions (fluxes) studied in relation to single crystal growth

System	Crystals	Remarks <sup>a</sup>	Ref.
<i>Oxidic compounds</i>			
Ga <sub>2</sub> O <sub>3</sub> -PbO		1	132, 133
Gd <sub>2</sub> O <sub>3</sub> -PbO		1	134
KNbO <sub>3</sub> -KBO <sub>2</sub>	KNbO <sub>3</sub>		135
NdP <sub>3</sub> O <sub>9</sub> -LiPO <sub>3</sub>	LiNdP <sub>4</sub> O <sub>12</sub>		136, 137
Sm(PO <sub>3</sub> ) <sub>3</sub> -KPO <sub>3</sub>	KSmP <sub>4</sub> O <sub>12</sub>		138
KGd(MoO <sub>4</sub> ) <sub>2</sub> -K <sub>2</sub> Mo <sub>2</sub> O <sub>7</sub>	KGd(MoO <sub>4</sub> ) <sub>2</sub>	2	139
LiGa(WO <sub>4</sub> ) <sub>2</sub> -Li <sub>2</sub> B <sub>2</sub> O <sub>4</sub>	LiGa(WO <sub>4</sub> ) <sub>2</sub> · Cr <sup>3+</sup>		140
MoO <sub>3</sub> -Bi <sub>2</sub> O <sub>3</sub>	Bi <sub>2</sub> O <sub>3</sub> xMoO <sub>3</sub>	3	141
PbFe <sub>0.5</sub> Nb <sub>0.5</sub> O <sub>3</sub> -PbO	PbFe <sub>0.5</sub> Nb <sub>0.5</sub> O <sub>3</sub>		142
PbMn <sub>0.5</sub> Nb <sub>0.5</sub> O <sub>3</sub> -PbO	PbMn <sub>0.5</sub> Nb <sub>0.5</sub> O <sub>3</sub>		143
Mn <sub>2</sub> O <sub>3</sub> -PbO	3PbO · 2Mn <sub>2</sub> O <sub>3</sub> 2MnO <sub>2</sub>	4	144
Sb <sub>2</sub> O <sub>3</sub> -PbO	PbSb <sub>2</sub> O <sub>6</sub> , Pb <sub>3+x</sub> Sb <sub>2</sub> O <sub>6+x</sub>	4	145
BaCO <sub>3</sub> -PbO	BaPbO <sub>3</sub>	4	146
Ba <sub>2</sub> PbO <sub>4</sub> -PbO	BaPbO <sub>3</sub>		146
BaB <sub>2</sub> O <sub>4</sub> -Na <sub>2</sub> O or Na <sub>2</sub> B <sub>2</sub> O <sub>4</sub>	BaB <sub>2</sub> O <sub>4</sub>	5	147
BaB <sub>2</sub> O <sub>4</sub> -NaCl, CaF <sub>2</sub> or Na <sub>2</sub> SO <sub>4</sub>	BaB <sub>2</sub> O <sub>4</sub>	5	148
<i>Chalcogenides and pnictides</i>			
In <sub>2</sub> S <sub>3</sub> -CdCl <sub>2</sub>	In <sub>2</sub> S <sub>3</sub>		149
CdIn <sub>2</sub> S <sub>4</sub> -CdCl <sub>2</sub>	CdIn <sub>2</sub> S <sub>4</sub>		
CdCr <sub>2</sub> Se <sub>4</sub> -Se	CdCr <sub>2</sub> Se <sub>4</sub>		150
CdCr <sub>2</sub> Se <sub>4</sub> -CdCl <sub>2</sub> + 2CdI <sub>2</sub>	CdCr <sub>2</sub> Se <sub>4</sub>		151
CdCr <sub>2</sub> Se <sub>4</sub> -CdCl <sub>2</sub> + PbCl <sub>2</sub>	CdCr <sub>2</sub> Se <sub>4</sub>		152
CdCr <sub>2</sub> Se <sub>4</sub> -CdCl <sub>2</sub>	CdCr <sub>2</sub> Se <sub>4</sub>		153
CuCr <sub>2</sub> Se <sub>4</sub> -CuI, CdCl <sub>2</sub> , NaCl, CuBr, PbCl <sub>2</sub> or PbCl <sub>2</sub> + CdCl <sub>2</sub>	CuCr <sub>2</sub> Se <sub>4</sub>		154
In <sub>2</sub> X <sub>3</sub> -InY <sub>3</sub>	InXY	X = Se, Te Y = Cl, Br, I	155
In <sub>2</sub> Te <sub>3</sub> -InBr <sub>3</sub>	InTeBr		156
CdGeP <sub>2</sub> -Ge -Cd	CdGeP <sub>2</sub>		157
CuGaS <sub>2</sub> -Pb -Sn	CuGaS <sub>2</sub> and by-products	Liquid miscibility gap	158
GaP, GaAs, InP or InAs-Pb	GaP, GaAs, InP or InAs	6	112
InP or InAs-Sn or Bi			
GaP-Bi or Sn	GaP	6	159
GaAs-Bi	GaAs		
GaAs-GaP-Sn	Ga(As,P)	7	160
Ga-In-As-Sb	(Ga,In)(As,Sb) layers	8	162
GaAs-Cr-Ga	GaAs · Cr		161
Al-Ga-In-As	(Al,Ga,In)As layers	8	163
Al-Ga-Sb	(Al,Ga)Sb	7	164
Pb-Sn-Te	(Pb,Sn)Te	9	165
Pb-Sn-Te	(Pb,Sn)Te	10	166

<sup>a</sup> 1, DTA data evaluated using model calculations. 2, Low temperature modification of KGd(MoO<sub>4</sub>)<sub>2</sub> 3, x = 1, 2 or 3. 4, Oxidation by air from the atmosphere. 5, Low temperature modification β-BaB<sub>2</sub>O<sub>4</sub> 6, Evaluation with the regular solution model. 7, Model calculations with DTA data. 8, Liquidus temperatures only by DTA. 9, Liquidus

which are in equilibrium with "123" below its decomposition temperature. The lowest melting (near eutectic) compositions in the bordering system BaO–CuO seemed to be the most promising solvents. Various DTA studies have given eutectic points at different compositions and temperatures: 18 mol% BaO, 820 °C [119]; 25 mol% BaO, 920 °C [120]; 28 mol% BaO, 926 °C in oxygen [121]; 33 mol% BaO, 950 °C in O<sub>2</sub> [122]; and 40 mol% BaO, 935 °C [118]. It is probable that the oxygen stoichiometry influenced these results, and a reversible phase transformation coupled with oxygen loss/gain around 900 °C was really established in Ba<sub>2</sub>Cu<sub>3</sub>O<sub>5-x</sub> [123].

Only the narrow temperature interval between the eutectic in the BaO–CuO border system and the peritectic decomposition of "123" and, consequently, a corresponding small concentration range can be used for growing single crystals of the "123" phase. From sections through the ternary Y<sub>2</sub>O<sub>3</sub>–BaO–CuO system as measured by DTA, Ba<sub>0.2 to 0.375</sub>CuO<sub>0.8 to 0.625</sub>O [124], Ba<sub>0.25</sub>Cu<sub>0.75</sub>O [125], Ba<sub>0.3</sub>Cu<sub>0.7</sub>O [120] and Ba<sub>0.33</sub>Cu<sub>0.67</sub>O [122] were suggested as favourable solvents.

In a comparison of rare earth compounds RBa<sub>2</sub>Cu<sub>3</sub>O<sub>7-x</sub> (R = La to Gd, Y) the highest incongruent melting temperature was found for the Nd compound (1085 °C [126]). Therefore this material should have a wider crystallization interval from a BaO–CuO flux than would YBa<sub>2</sub>Cu<sub>3</sub>O<sub>7-x</sub>; crystal growth has been demonstrated in this system. The wider interval of primary crystallization of the Nd–"123" phase as compared to the Y–"123" one was confirmed in the pseudobinary section with the solvent Ba<sub>0.375</sub>Cu<sub>0.625</sub>O [127], resulting in successful single crystal growth [128]. In the corresponding system with Er<sub>2</sub>O<sub>3</sub>, crystallization onset was detected from DTA cooling curves at 1000 °C with no hint of undercooling. Using this temperature as a maximum in crystal growth experiments gave crystals of the ErBa<sub>2</sub>Cu<sub>3</sub>O<sub>7-x</sub> phase [129].

Superconducting materials in the Bi–Ca–Sr–Cu–O and Tl–Ca–Ba–Cu–O systems exhibit higher critical temperatures than those mentioned previously. Liquidus temperatures in these quinary systems are lower than in rare earth–alkaline earth–copper oxide systems. Thus, problems of crucible corrosion and oxygen non-stoichiometry may be reduced. However, the phase relationships are very complicated. Nevertheless preliminary DTA studies on pseudobinary sections Bi<sub>n</sub>CaSrCu<sub>3-n</sub>O<sub>y</sub> (1 ≤ n ≤ 2) [130] and Tl<sub>2</sub>Ba<sub>2</sub>CuO<sub>x</sub>–Tl<sub>2</sub>Ca<sub>3</sub>Ba<sub>2</sub>Cu<sub>4</sub>O<sub>y</sub> [131] proved useful in establishing conditions for successful growth of Bi<sub>2</sub>(Sr,Ca)<sub>3</sub>Cu<sub>2</sub>O<sub>8</sub> and Tl<sub>2</sub>Ca<sub>1-n</sub>Ba<sub>2</sub>Cu<sub>n</sub>O<sub>z</sub> single crystals.

Other DTA studies on phase equilibria that are relevant to crystal growth from high temperature solutions are listed in Table 2.

DTA can be useful for investigating vapour–liquid–solid reactions involving A(III)B(V) compounds. The reaction of molten gallium with an AsCl<sub>3</sub>–H<sub>2</sub> gas mixture was studied by Koukitu and Seki [167] at constant temperature. After an induction period necessary to saturate the melt with arsenic,

an exothermic peak occurred coinciding with the appearance of a GaAs crust on the melt surface.

Roy and co-workers [168–172] have tried to estimate by means of DTA the kinetic parameters of the crystallization from high-temperature solutions. The partial area method applied to the DTA cooling curve gave the degree of crystallization at time  $t$  as

$$\alpha_t = A_t/A_{\text{total}}$$

where  $A_t$  is the partial area under the DTA peak from onset to time  $t$ , and  $A_{\text{total}}$  is the total area of the DTA peak. Plots of  $\alpha_t$  can then be calculated for DTA diagrams of one system, e.g.  $\text{Na}_2\text{WO}_4(\text{solvent})-\text{CaWO}_4(\text{solute})$  at different concentrations and with different cooling rates  $\bar{\beta}$ . From the dimensions of the crystals, e.g. their final length as determined by microscopic measurements after the DTA experiment, their length at any time during growth  $l_t$  can be estimated from

$$(l_t/l_{\text{final}})^3 = \alpha_t$$

A plot of  $l_t$  vs.  $t$  allows a calculation of  $dl/dt$ , which is related to the diffusion rate constant  $k_D$  for growth along the main crystal axis.

$$k_D = (dl/dt)_0^2/2a\bar{\beta}$$

Here  $(dl/dt)_0$  is the length change at the beginning of crystallization, determined by extrapolation of  $l$  vs.  $t$  to  $t=0$ , and  $a$  is a temperature development of excess solute concentration calculated from the liquidus curve of the system, previously evaluated from DTA curves.

It has been shown that  $k_D$  increases at increasing initial crystallization temperature,  $T$  (800–1000 °C) and increasing cooling rates,  $\bar{\beta}$  (40–200 K h<sup>-1</sup>) by more than one order of magnitude. This  $k_D$  is valid at the onset of crystallization, but at later stages of crystallization convection is retarded by the decreasing free space remaining between the crystallites in the unstirred melt.

The temperature dependence of  $k_D$  can be used to estimate an activation energy,  $E$ , from an Arrhenius plot [169]

$$k_D = k_0 \exp(-E/RT)$$

$$\ln k_D = \ln k_0 - E/RT$$

The linearity of this plot confirms that the crystallization of  $\text{CaWO}_4$  from molten  $\text{Na}_2\text{WO}_4$  is a diffusion-controlled process.

A similar evaluation procedure applied to the crystallization [170] of  $\text{SrWO}_4$  and  $\text{BaWO}_4$  has shown that measurable crystal growth [171,172] occurred after a certain induction period  $t_i$ , during which only nuclei were formed. Crystallization commenced at some critical supersaturation  $\Delta C_i$ ,

again as a diffusion-controlled process. From  $\Delta C_i$ ,  $T_i$  and  $t_i$  a rate constant  $k_n$  for the heterogeneous nucleation can be estimated.

#### CONCLUDING REMARKS

The technique of DTA has one main limitation: whilst it shows that something occurs at a certain temperature and allows the heat and the progress of the phenomenon under study to be estimated, it does not provide any direct evidence of what actually happens. This limitation is a relative one because the shape of the thermal effects and their dependence on the chemical composition and other adjustable variables and even a visual inspection of the sample after the DTA run enable the thermoanalyst to draw his/her conclusions. Nevertheless, it must be emphasized that DTA results need to be complemented and confirmed by results obtained with other techniques of investigation applied either in situ, under programmed temperature and, preferably, simultaneously with DTA (on the same sample), e.g. thermogravimetry or thermomicroscopy [173], or a posteriori, i.e. studying the samples after DTA measurement and cooling to room temperature, e.g. phase analysis by X-ray diffraction, spectroscopic or metallographic techniques.

Although not explicitly mentioned, most of the works cited in the present paper have made use of such techniques to understand and/or complement the DTA results.

This review covers studies concerned with the material to be transformed into single crystals, without using single-crystal samples. Hence fundamental information on the relevant systems is obtained before producing the first single crystal. However, the single crystals obtained from a growth procedure may also be characterized using DTA and this provides indirect information on the growth process. In the case of lithium niobate mentioned previously, the Curie temperature,  $T_C$ , depends strongly on the lithium content  $x$  in  $\text{Li}_{1-x}\text{Nb}_{1+x}\text{O}_{3+2x}$ . Careful DTA measurements of the  $T_C$  of as-grown crystals as dependent on melt stoichiometry and growth conditions, compared to the  $T_C$  of the frozen melt before and after the growth procedure, have been used to determine the congruently melting composition [174,175] and to monitor the effect of dopants on crystal growth.

However, such DTA investigations of single crystals are connected with solid state physics and possibly the application of the material, and are thus not treated in detail here. Other thermoanalytical techniques such as the variants of thermoelectrometry, thermomagnetometry, thermoptometry and thermoluminescence (frequently not named by these terms) are more established in terms of the study of single crystals, because they are more closely related to possible or real applications.

Returning to DTA, comparing the applications of this method described in the literature and reviewed here with the potential applications listed in

the introduction to this article, it can be seen that the range of utility of DTA is far from exhausted. Thus it can be predicted that the worldwide increase in work concerned with the preparation, investigation and application of single crystals on the one hand and the development of DTA instrumentation and methods of evaluation on the other will together stimulate further progress in this field.

## REFERENCES

- 1 S Haussühl, J. Eckstein, K Recker and F Wallrafen, *J Cryst Growth*, 40 (1977) 200
- 2 A.A Kaminski, B V. Mill, G.G. Khodzhabayyan, A.F. Konstantinova, A I Okorochkov and I M Silvestrova, *Phys Status Solidi A*, 43 (1977) 71
- 3 F Wallrafen, J. Eckstein and K Recker, *Krist Tech*, 10 (1975) K101.
- 4 O F. Hill and J.C. Brice, *J Mat Sci.*, 9 (1974) 1252
- 5 A.A. Ballman and H. Brown, *J. Cryst Growth*, 41 (1977) 36.
- 6 K Wacker and P. Buck, *Cryst. Res Technol.*, 20 (1985) 1025.
- 7 A C Pastor, *Mat Res Bull*, 20 (1985) 1165.
- 8 N Rakhimov, B M Zhigarnovskii, Yu.M. Polyakov, V Yu Kozhenkov, V.S Karapetyan, G O Takanashvili and G.N Moisashvili, *Izv Akad Nauk. SSSR Ser. Neorg. Mater.*, 21 (1985) 1095
- 9 V A Vinokurov and P.V Klevtsov, *Kristallografiya*, 17 (1972) 127
- 10 K Nassau, H.J. Levinstein and G.M. Loiacono, *J Phys. Chem Solids*, 26 (1965) 1805.
- 11 T. Yamada and H. Koizumi, *J. Cryst Growth*, 64 (1983) 558.
- 12 D.A Jones and W A. Shand, *J Cryst Growth*, 2 (1968) 361
- 13 F H. Spedding, B J. Beaudry, D.C. Henderson and J Moorman, *J. Chem Phys*, 60 (1974) 1578
- 14 R.C. Pastor and M. Robinson, *Mat Res. Bull*, 9 (1974) 569
- 15 B.P Sobolev, P.P. Fedorov, D B Shteynberg, B.V. Smitsyn and G S Shakhkalamian, *J. Solid State Chem.*, 17 (1976) 191.
- 16 B.P. Sobolev, P.P Fedorov, K B Serranian and N.L Tkachenko, *J Solid State Chem.*, 17 (1976) 201
- 17 G Garton and P.J Walker, *Mat. Res Bull*, 17 (1982) 1227
- 18 B.P Sobolev and N L. Tkachenko, *J Less-Common Metals*, 85 (1982) 155
- 19 A.A Kaminski, B.P. Sobolev, S E. Sarkisov, G.A Denisenko, V.V. Ryabchenkov, V.A Fedorov and T V Uvarova, *Izv. Akad. Nauk USSR, Ser Neorg. Mater.*, 18 (1982) 482
- 20 F Wallrafen and K Recker, *Z Kristallogr*, 136 (1978) 135
- 21 B V. Mill', M.V. Levandov and K P Belov, *Izv Akad Nauk SSSR, Ser. Neorg Mater.*, 15 (1979) 1811
- 22 J.P M Damen, J.A Pistorius and J M Robertson, *Mat Res Bull.*, 12 (1977) 73.
- 23 B V Mill', A V. Butashin, A M. Ellern and A.A Majer, *Izv. Akad. Nauk USSR, Ser. Neorg. Mater.*, 17 (1981) 1648.
- 24 K Megumi, H. Yumoto, S. Ashida, S Akiyama and Y. Furuhashi, *Mat. Res Bull.*, 9 (1974) 391.
- 25 I.A Ivanova, A M. Morozov, M A Petrova, I.G Podkolzina and P.P. Feofilov, *Izv Akad Nauk USSR, Ser. Neorg Mater*, 11 (1975) 2175.
- 26 R.C Pastor, M. Robinson and W.M. Akutagawa, *Mat Res. Bull.*, 10 (1975) 501
- 27 H. Safi, I.R. Harris, B. Cockayne and J.G Plant, *J. Mat. Sci.*, 16 (1981) 3203.
- 28 I R Harris, H. Safi, N.A Smith, M. Altunbas, B. Cockayne and J.G Plant, *J Mat Sci.*, 18 (1983) 1235.

- 29 A Reisman and F. Holtzberg, *J. Am. Chem. Soc.*, 80 (1958) 6503.
- 30 U Flückiger and H. Arend, *J Cryst Growth*, 43 (1978) 406.
- 31 W Xing, H. Looser, M. Wüest and H. Arend, *J Cryst. Growth*, 78 (1986) 431
- 32 M V Mokhosoev, I F. Kokot and I S. Kononenko, *Zh. Neorg. Khim.*, 15 (1970) 1684
- 33 A.A. Kaminski, S.E. Sarkisov, J. Bohm, P. Reiche, D. Schultze and R. Uecker, *Phys Status Solidi A*, 43 (1977) 71.
- 34 A A Evdokimov, A.A. Eliseev, V A. Murashov and G P Khomchenko, *Zh Neorg Khim.*, 26 (1981) 3089.
- 35 P V. Klevtsov and V.A. Vinokurov, *Izv Akad Nauk USSR, Ser. Neorg Mater.*, 11 (1975) 387
- 36 I D Turyanitsa, I D. Olekseyuk and I.I. Kozmanko, *Izv. Akad. Nauk. SSSR, Ser Neorg. Mater.*, 9 (1973) 1433
- 37 G. Offergeld and J van Cakenberghe, *J Phys Chem Solids*, 11 (1959) 310
- 38 D Schultze and R Uecker, *Thermochim Acta*, 93 (1985) 509
- 39 P Bohac and P Kaufmann, *Mat Res. Bull.*, 10 (1975) 613
- 40 V.B. Lazarev, G.A. Sharpataya, Z P. Ozerova, K A. Sokolovskii and S.F. Marenkin, *Izv. Akad. Nauk SSSR, Ser. Neorg. Mater.*, 22 (1986) 1204
- 41 V T. Gabrielian, L.M. Fedorova, E B. Tkachenko, A.Y. Neiman and N S Nikogostian, *Cryst. Res. Technol.*, 21 (1986) 439
- 42 A Reisman and F Holtzberg, *J. Am Chem. Soc.*, 80 (1958) 6503.
- 43 P. Lerner, C. Legras and J.P. Dumas, *J Cryst. Growth*, 3 (1868) 231
- 44 J R Carruthers, G.E. Peterson, M. Grasso and P.M. Bridenbaugh, *J. Appl. Phys.*, 42 (1971) 1845
- 45 J R Carruthers and M. Grasso, *J Electrochem Soc.*, 117 (1970) 1426
- 46 K. Megumi, K. Nagatsuma, Y. Kashwada and Y. Furuhashi, *J Mat. Sci.*, 11 (1976) 1583
- 47 B A Scott, E.A. Giesse and D F O'Kane, *Mat. Res. Bull.*, 4 (1969) 107
- 48 J R. Carruthers and M. Grasso, *Mat. Res. Bull.*, 4 (1969) 413.
- 49 K.G. Barraclough, I.R. Harris, B. Cockayne, J.G. Plant and A.W. Vere, *J Mat. Sci.*, 5 (1970) 389
- 50 T Sugai and M. Wada, *Jpn. J Appl Phys.*, 11 (1972) 1863
- 51 T Sugai, *Jpn J Appl. Phys.*, 25 (1986) 792.
- 52 V Krämer, H Matthes and A Marshall, *J. Mat Sci.*, 10 (1975) 547
- 53 P.P. Fedorov, Yu.G. Sizganov, B.P. Sobolev and M. Shvanner, *J Therm. Anal.*, 8 (1975) 239
- 54 K. Recker and F. Wallrafen, *Ber Dtsch Keram. Ges.*, 50 (1973) 68.
- 55 P P Fedorov and B P. Sobolev, *Kristallografiya*, 20 (1975) 763, *J Less-Common Met.*, 63 (1979) 31
- 56 B P. Sobolev and P P Fedorov, *J Less-Common Met.*, 60 (1978) 33.
- 57 B P Sobolev and K.B. Seiranyan, *Kristallografiya*, 20 (1975) 763.
- 58 B P Sobolev and K.B. Seiranyan, *J Solid State Chem.*, 39 (1981) 337
- 59 V A Gorbulev, P P. Fedorov and B.P. Sobolev, *J Less-Common Met.*, 76 (1980) 55
- 60 E Yu Peresh, L.S. Shnyrko, V.I. Tkachenko, V I Starosta, A.A. Kikineshu, K.A. Batori and V S. D'ordya, *Zh Neorg Khim.*, 27 (1982) 473.
- 61 V B. Lazarev, E.Yu. Peresh, V.I. Starosta and V V. Mudryi, *Zh. Neorg. Khim.*, 30 (1985) 1502
- 62 D A Nelson, C.J. Summers and C.R. Whittsett, *J. Electron. Mat.*, 6 (1977) 507
- 63 F R. Szofran and S.L. Lehoczky, *J Electron. Mat.*, 10 (1981) 1131; 12 (1983) 713
- 64 R K Route, R.S. Feigelson and R J. Raymakers, *J Cryst Growth*, 24/25 (1974) 390.
- 65 J.C. Mikkelsen, *Mat. Res. Bull.*, 12 (1977) 497
- 66 M Kokta, J.R. Carruthers, M. Grasso, H M Kasper and B. Tell, *J. Electron. Mat.*, 5 (1976) 69
- 67 J.C. Mikkelsen, *J. Electron Mater.*, 10 (1981) 541

- 68 J.J.M Binsma, J.L. Giling and J. Bloem, *J. Cryst. Growth*, 50 (1980) 429.
- 69 A.W. Verheijen, L.J. Giling and J. Bloem, *Mat. Res. Bull.*, 14 (1979) 237.
- 70 I.V. Bodnar, A.P. Bologa and B.V. Korzun, *Krist. Tech.*, 15 (1980) 1285
- 71 J. Cornet and D. Rossier, *Mat. Res. Bull.*, 8 (1973) 9.
- 72 V. Krämer, *J. Therm. Anal.*, 16 (1979) 295.
- 73 V. Krämer and K. Berroth, *Mat. Res. Bull.*, 15 (1980) 299
- 74 V. Krämer, *Thermochim. Acta*, 15 (1976) 205.
- 75 J. Strassburger, *J. Electrochem. Soc.*, 116 (1969) 640.
- 76 M.C. Allibert, C. Chatillon, J. Mareschal and F. Lissalde, *J. Cryst. Growth*, 23 (1974) 289
- 77 M.A. DiGiuseppe and S. Soled, *J. Solid State Chem.*, 30 (1979) 203
- 78 M.A. DiGiuseppe, S.L. Soled, W.M. Wenner and J.E. Macur, *J. Cryst. Growth*, 49 (1980) 746
- 79 J.L. Caslavsky and D.J. Viechnicki, *J. Mat. Sci.*, 15 (1980) 1709
- 80 V.I. Psarev, V.A. Andronnikov and A.L. Ivanov, *Izv. Akad. Nauk SSSR, Ser. Neorg. Mater.*, 20 (1984) 1449
- 81 G. Corsmit, M.A. van Driel, R.J. Elsenaar, W. van de Guchte, A.M. Hoogenboom and J.C. Sens, *J. Cryst. Growth*, 75 (1986) 551.
- 82 K. Hirota and T. Sekine, *Bull. Chem. Soc. Jpn.*, 52 (1979) 1368.
- 83 T.M. Yanushkevich, A.V. Gur'ev and F.M. Musalimov, *Zh. Neorg. Khim.*, 23 (1978) 3306
- 84 O. Yamaguchi, K. Sugura, M. Muto and K. Shimizu, *Z. Anorg. Allg. Chem.*, 525 (1985) 230
- 85 D. Elwell, B.W. Neate and S.H. Smith, *J. Therm. Anal.*, 1 (1969) 319.
- 86 B.W. Neate, D. Elwell, H.S. Smith and D.M. Agostino, *J. Phys. E. Sci. Instrum.*, 4 (1971) 775.
- 87 K. Fischer, *Krist. Tech.*, 11 (1976) 635
- 88 B.M. Wanklyn and B.E. Watts, *Mat. Res. Bull.*, 19 (1984) 711
- 89 B.M. Wanklyn, B.E. Watts and V.V. Fenin, *J. Cryst. Growth*, 70 (1984) 459.
- 90 B.M. Wanklyn, H. Dabkowska and B.E. Watts, *Mat. Res. Bull.*, 21 (1986) 1175
- 91 M. Tmar, A. Gabriel, C. Chatillon and I. Ansara, *J. Cryst. Growth*, 68 (1984) 557
- 92 K. Imai, K. Suzuki, T. Haga, Y. Hasegawa and Y. Abe, *J. Cryst. Growth*, 54 (1981) 501.
- 93 G.S. Olejnik, P.A. Mizetski, A.I. Nizkova, L.A. Polvtsev and I.A. Ryadine, *Izv. Akad. Nauk USSR, Ser. Neorg. Mater.*, 19 (1983) 1799
- 94 G.S. Olejnik and P.A. Mizetski, *Izv. Akad. Nauk USSR, Ser. Neorg. Mater.*, 20 (1984) 1490
- 95 W. Eigermann, G. Müller-Vogt and W. Wendl, *Phys. Status Solidi A*, 49 (1978) 145
- 96 M.L. Sholokhovitch and V.E. Dugin, *Izv. Akad. Nauk USSR, Ser. Neorg. Mater.*, 20 (1984) 300.
- 97 I.V. Ivannikova, K.E. Mironov and A.A. Pavlov, *Zh. Neorg. Khim.*, 32 (1987) 180
- 98 A. Baudrant, H. Vial and J. Daval, *Mat. Res. Bull.*, 10 (1975) 1373
- 99 J. Hemmerling, K. Fischer and E. Sinn, *Cryst. Res. Technol.*, 16 (1981) 413
- 100 S. Kondo, S. Miyazawa, S. Fushimi and K. Sugu, *Appl. Phys. Lett.*, 26 (1975) 489.
- 101 R.S. Madoyan, G.N. Sarkisyan, Yu.G. Petrosyan and O.A. Khachaturyan, *Zh. Neorg. Khim.*, 24 (1979) 3088.
- 102 R.R. Neurgaonkar, M.H. Kalisher, E.J. Staples and T.C. Lim, *Appl. Phys. Lett.*, 35 (1979) 606
- 103 R.S. Madoyan, G.N. Sarkisyan and O.A. Khachaturyan, *Cryst. Res. Technol.*, 20 (1985) 1031
- 104 S. Kondo, K. Sugu, S. Miyazawa and S. Uehara, *J. Cryst. Growth*, 46 (1979) 314
- 105 H.D. Jonker, *J. Cryst. Growth*, 28 (1975) 231.
- 106 P. Görnert and C.G. D'Ambly, *Phys. Status Solidi A*, 29 (1975) 95.

- 107 K. Fischer, *Krist. Tech*, 11 (1979) 635.
- 108 K. Fischer and P. Görnert, *Cryst. Res Technol*, 17 (1982) 775
- 109 J. Sarai, M. Kitagawa, M. Ishida and T. Tanaka, *J. Cryst Growth*, 43 (1987) 13
- 110 S.R. Sashital, *J. Cryst. Growth*, 71 (1985) 33.
- 111 S.R. Sashital, *J. Cryst Growth*, 74 (1986) 203
- 112 A. Leonhardt and G. Kühn, *J. Less-Common Met.*, 39 (1975) 247.
- 113 G. Kühn and A. Leonhardt, in H.G. Schneider (Ed.), *Advances in Epitaxy and Endotaxy*, Akademiai Kiado, Budapest, 1976, pp. 213–255.
- 114 K. Oka and H. Unoki, *Jpn J. Appl. Phys.*, 26 (1987) L1590.
- 115 C. Chen, B.E. Watts, B.M. Wanklyn, P.A. Thomas and P.W. Haycock, *J. Cryst. Growth*, 91 (1988) 659.
- 116 P.J. Picone, H.P. Jenssen and D.R. Gabbe, *J. Cryst. Growth*, 91 (1988) 463.
- 117 K. Oka and H. Unoki, *Jpn J. Appl. Phys.*, 28 (1989) L937
- 118 H.J. Scheel, *Physica C*, 153–155 (1988) 44.
- 119 A.B. Bykov, L.N. Demianets, I.P. Zibrov, G.V. Kanunnikov, O.K. Melnikov and S.M. Stushov, *J. Cryst. Growth*, 91 (1988) 302
- 120 M. Maeda, M. Kadoi and T. Ikeda, *Jpn. J. Appl. Phys.*, 28 (1989) 1417
- 121 M. Nevřiva, E. Pollert, L. Matejková and A. Třiska, *J. Cryst Growth*, 91 (1988) 434
- 122 S. Nomura, H. Yoshino and K. Ando, *J. Cryst. Growth*, 92 (1988) 682
- 123 I. Halász, V. Fulop, I. Kirschner and T. Porjesz, *J. Cryst Growth*, 91 (1988) 444.
- 124 K. Oka, K. Nakane, M. Ito, M. Saito and H. Unoki, *Jpn J. Appl. Phys.*, 27 (1988) L1065.
- 125 K. Fischer, R. Hergt and D. Linzen, *Cryst. Res. Technol*, 23 (1988) 1169.
- 126 A. Katsui, Y. Hidaka and H. Ohtsuka *Jpn J. Appl. Phys.*, 26 (1987) L1521.
- 127 K. Oka and H. Unoki, *J. Cryst. Growth*, 99 (1990) 922
- 128 K. Oka, M. Saito, M. Ito, K. Nakane, K. Murata, Y. Nishihara and H. Unoki, *Jpn. J. Appl. Phys.*, 28 (1989) L219.
- 129 B.M. Wanklyn, C. Chen, P.A.J. de Groot and G.P. Rapson, *Supercond. Sci Technol*, 2 (1989) 129.
- 130 K. Tomomatsu, A. Kurosaka, H. Tominaga, T. Takayama, O. Fukuda and H. Osanai, *Appl. Phys. Lett.*, 55 (1989) 298.
- 131 T. Kotani, T. Kaneko, H. Takei and K. Tada, *Jpn. J. Appl. Phys.*, 28 (1989) L1378.
- 132 M. Nevřiva, E. Pollert and K. Fischer, *Mat. Res Bull.*, 13 (1978) 473
- 133 M. Nevřiva, E. Pollert and K. Fischer, *Thermochim. Acta*, 34 (1979) 85.
- 134 M. Nevřiva, E. Pollert and K. Fischer, *Mat. Res Bull.*, 15 (1980) 1073
- 135 L.M. Rudkovskaya and V.G. Samotrakov, *Izv. Akad. Nauk. USSR, Ser. Neorg. Mater.*, 16 (1980) 55.
- 136 J. Nakano and T. Yamada, *J. Am. Ceram. Soc.*, 59 (1976) 172.
- 137 J. Nakano, T. Yamada and S. Miyazawa, *J. Am. Ceram. Soc.*, 62 (1979) 465.
- 138 M. Ferid, N.K. Arigub and M. Trabelsi, *J. Solid State Chem.*, 69 (1987) 1
- 139 L.P. Kozeeva and A.A. Pavlyuk, *Izv. Akad. Nauk, Ser. Neorg. Mater.*, 19 (1983) 1730
- 140 G. Wang, Z. Luo and J. Chen, *J. Cryst. Growth*, 100 (1990) 447
- 141 T. Chen and G.S. Smith, *J. Solid State Chem.*, 13 (1975) 288.
- 142 I.H. Brunskill, P. Tissot and H. Schmid, *Thermochim. Acta*, 49 (1981) 351.
- 143 I.H. Brunskill, R. Boutellier, W. Depmeier, H. Schmid and H.J. Scheel, *J. Cryst. Growth*, 56 (1982) 541.
- 144 A.A. Bush, A.V. Titov, B.I. Al'shin and Yu.I. Venevtsev, *Zh. Neorg. Khim.*, 22 (1977) 2238.
- 145 A.A. Bush and Yu.I. Venevtsev, *Zh. Neorg. Khim.*, 23 (1978) 2195.
- 146 K. Oka and H. Unoki, *Jpn J. Appl. Phys.*, 23L (1984) 770.
- 147 Huang Q. and Liang J., *Acta Phys. Sin.*, 30 (1981) 559.
- 148 Huang Q. and J. Liang, *J. Cryst. Growth*, 97 (1989) 720.

- 149 V.P. Buzhor, R.Yu. Lyalikova, S.I. Radautsan, S.A. Ratseev and V.E. Tezlevan, *Izv. Akad. Nauk USSR, Ser. Neorg. Mater.*, 21 (1985) 498.
- 150 G.G. Shabunina, N.P. Luzhnaya and V.T. Kalinnikov, *Zh. Neorg. Khim.*, 26 (1981) 476.
- 151 G.G. Shabunina, N.P. Luzhnaya, G.I. Vinogradova and T.G. Aminov, *Izv. Akad. Nauk USSR, Ser. Neorg. Mater.*, 17 (1981) 1727
- 152 G.G. Shabunina, N.M. Shibanova, T.G. Aminov and V.T. Kalinnikov, *Zh. Neorg. Khim.*, 34 (1989) 1586.
- 153 M. Berkowski and W. Piekarczyk, *J. Cryst. Growth*, 40 (1977) 253
- 154 M.A. Chernitsyna, V.T. Kallnikov, A.A. Babitsyna and T.A. Emel'yanova, *Zh. Neorg. Khim.*, 23 (1978) 77
- 155 R. Knep, A. Wilms, H.H. Beister and K. Syassen, *Z. Naturforsch., Teil B*, 36 (1981) 1520
- 156 R. Knep and A. Wilms, *Mat. Res. Bull.*, 15 (1980) 763.
- 157 M. Boiko, A.S. Korshchevskii and Yu.K. Undalov, *Izv. Akad. Nauk USSR, Ser. Neorg. Mater.*, 12 (1976) 761.
- 158 H.J. Hoebler, G. Kühn and A. Tempel, *J. Cryst. Growth*, 53 (1981) 131.
- 159 A. Leonhardt and G. Kuhn, *Krist. Techn.*, 9 (1974) 77
- 160 H. Rentsch, G. Kühn, A. Leonhardt, V. Gottschalch and E. Butter, *Krist. Techn.*, 11 (1976) 133
- 161 M.D. Deal, R.A. Gasser and D.A. Stevenson, *J. Phys. Chem. Solids*, 46 (1985) 859
- 162 K. Nakajima, K. Osamura, K. Yasuda and Y. Murakami, *J. Cryst. Growth*, 41 (1977) 87
- 163 K. Nakajima, K. Osamura and Y. Murakami, *J. Electrochem. Soc.*, 122 (1975) 1245.
- 164 K. Osamura, J. Inoue, K. Nakajima and Y. Murakami, *J. Electrochem. Soc.*, 126 (1979) 1992
- 165 A.P. Petukhov, Yu.V. Andreev and A.O. Olesk, *Izv. Akad. Nauk USSR, Ser. Neorg. Mater.*, 16 (1980) 55
- 166 V.F. Mikhailov, O.V. Pelevin, A.M. Sokolov and A.M. Khorvat, *Izv. Akad. Nauk USSR, Ser. Neorg. Mater.*, 14 (1978) 777.
- 167 A. Koukitu and H. Seki, *J. Cryst. Growth*, 67 (1984) 549
- 168 B.N. Roy and S. Appalasami, *J. Therm. Anal.*, 16 (1979) 27
- 169 B.N. Roy and Kim Hong Goh, *J. Therm. Anal.*, 18 (1980) 427.
- 170 B.N. Roy, S. Appalasami and A.K. Chatterji, *Cryst. Res. Technol.*, 16 (1981) 329
- 171 B.N. Roy, S. Appalasami and Kim Hong Goh, *J. Therm. Anal.*, 20 (1981) 379
- 172 B.N. Roy and M.R. Roy, *Cryst. Res. Technol.*, 17 (1982) 167.
- 173 D. Schultze, *Thermochim. Acta*, 29 (1979) 233.
- 174 H.M. O'Bryan, P.K. Gallagher and C.D. Brandle, *J. Am. Ceram. Soc.*, 68 (1985) 493.
- 175 P.K. Gallagher, H.M. O'Bryan and C.D. Brandle, *Thermochim. Acta*, 133 (1988) 1